PRELIMINARY MODEL STUDIES OF SINKING PLUMES

By Ingrid Bork

SMHI Rapporter
HYDROLOGI OCH OCEANOGRAFI
Nr RHO 14 (1978)

SVERIGES METEOROLOGISKA OCH HYDROLOGISKA INSTITUT

PRELIMINARY MODEL STUDIES OF SINKING PLUMES

By Ingrid Bork

SMHI Rapporter
HYDROLOGI OCH OCEANOGRAFI
Nr RHO 14 (1978)

INLEDANDE MODELLSTUDIER AV SJUNKANDE KYLVATTENPLYMER

SVERIGES METEOROLOGISKA OCH HYDROLOGISKA INSTITUT
Norrköping 1978
ISSN 0347-7827

ABSTRACT

The hydrodynamic equations are reviewed and simplified for use in a study of sinking cooling water plumes. Two examples of observed sinking plumes are shown. A numerical model is employed to study the magnitude of different terms in the equations and the effect of varying turbulent diffusion coefficients. The model is a two dimensional one (one horizontal and one vertical dimension). It is concluded that the sinking phenomena is very sensitive to changes in the vertical diffusion coefficient and it is recomended that future three dimensional studies are carried out in a model containing a reliable computation of the turbulent fluxes.

CONTENTS

PROBLEM AND OBSERVATIONS

The density of water is a function of both temperature and salinity. For salinities less then 24 ‰ there exists a density maximum for a temperature above the freezing point. Therefore, water-discharges into ambient water at freezing temperature will sink down towards the bottom if they are cooled below T (ρ max).

Fig 1 shows ρ_t values for S = 0 ‰ . In fresh water the stratification of a water column with a linear temperature gradient from 8 °C at the upper boundary and 0 °C at the bottom would be unstable between 0 °C and 4 °C and stable between 4 °C and 8 °C.

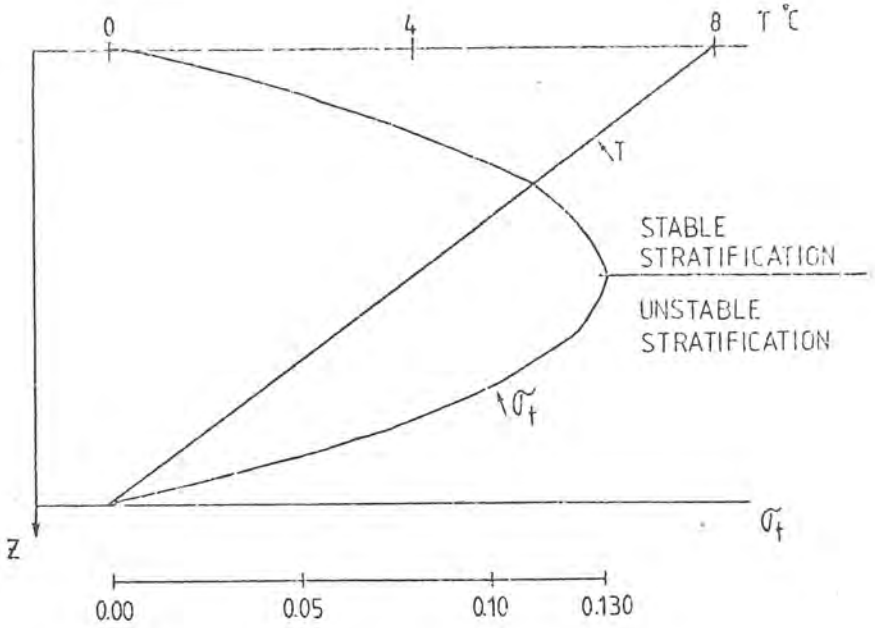

Figure 1 Density stratification for a linear temperature stratification (salinity = 0 ‰) $\sigma_t=(\rho-1)\ 10^3$.

The range in which sinking can be observed decreases with salinity (compare fig 2). Although the freezing point temperature becomes negativ for salt water, no pronounced sinking is to be expected for salinities above about 15 ‰ . Sinking plumes have been observed in the Baltic

at salinities of about 7 to 8 ‰ .

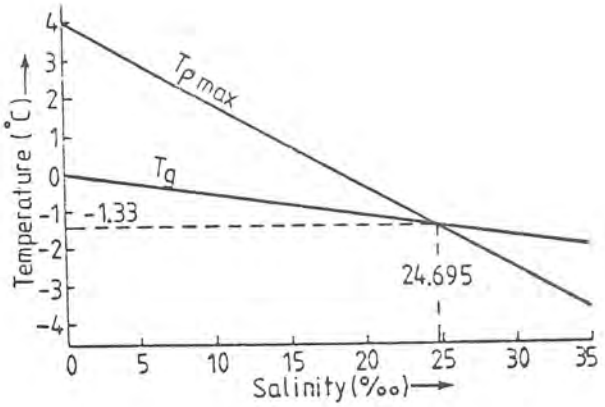

Figure 2 Temperature of the density maximum $T_{\rho\ max}$ and temperature of the freezing point, tg, for sea water of different temperature.

A rewiew of sinking plumes observed by SMHI is given by Vasseur (1976). Fig 3 and 4 show two typical examples. A characteristic of a sinking plume is that it is narrow at the surface compared to floating plumes but spreads along the bottom.

Sinking is, however, not always observed under winter conditions, even if temperature and salinity distribution indicate instability, according to the condition for static stability:

$$\frac{1}{\rho}\frac{d\rho}{dz} = \frac{1}{\rho}\frac{\partial\rho}{\partial s}\frac{ds}{dz} + \frac{1}{\rho}\frac{\partial\rho}{\partial T}\frac{dT}{dz} < 0 \quad \text{(z positiv downward)}$$

In fact, instability associated with vertical overturning of water masses is more complicated, as heat conduction, friction and diffusion retard to the motion and tend to stabilize it (Turner 1973). The two non-dimensional numbers governing the process are the Rayleigh number, which is for parallel plate convection

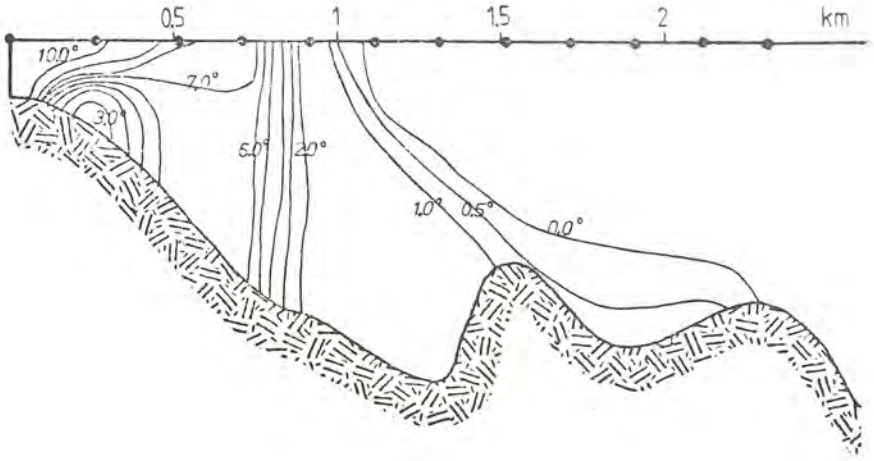

Figure 3 Example of a sinking plume outside Oskarshamnsverket on the south-east coast of Sweden.

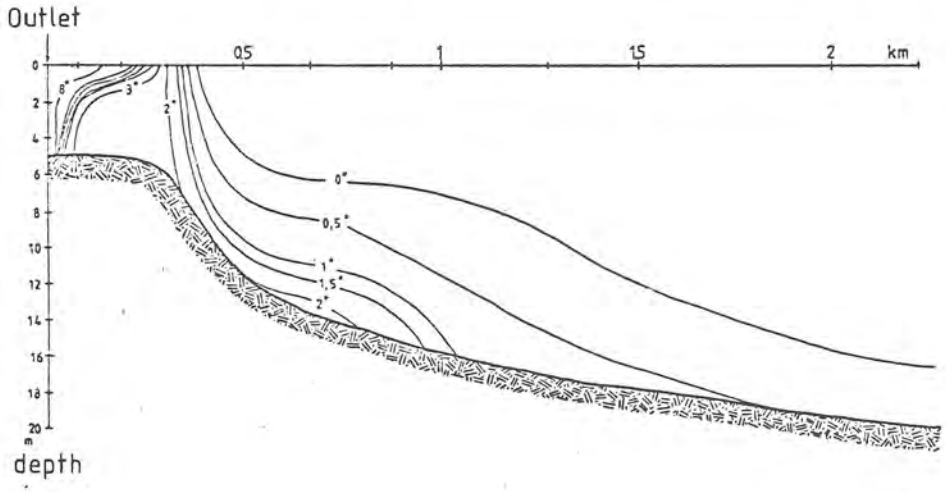

Figure 4 Example of a sinking plume outside Oskarshamnsverket on the south-east coast of Sweden.

and constant salinity defined as

$$Ra = g \beta \Delta T H^3 / \kappa_T \nu$$

with $\beta = -\frac{1}{\rho}\frac{\partial \rho}{\partial T}$, ΔT temperature difference between plates separated by a distance H and the Prandtl number $Pr = \nu / \kappa_T$. In the case of parallel plate convection a critical Rayleigh number can be determined at which instability occurs (compare Stern 1975). On the basis of this stability criterion Neumann (compare Neumann, Pierson 1966) has indicated that neutral stratification in the ocean can occur only when the vertical density gradient reaches a certain negative value, or when

$$-\frac{1}{\rho}\frac{\partial \rho}{\partial S}\frac{dS}{dz} \quad -\frac{1}{\rho}\frac{\partial \rho}{\partial T}\frac{dT}{dz} > \text{const.}\ \frac{1}{\rho^2 g}\frac{AK}{h^4}$$

where A and K are turbulent viscosity and turbulent heat conductivity respectively, and h is the thickness of the layer where negative density gradients occur. The constant is in the order of 10^3 in oceans. A corresponding value for the Baltic Sea is not available.

There are quite a lot of studies on convection, concerning simplified cases like vertical convection which arises when a broad horizontal layer is heated uniformly from below and cooled from above (compare Turner 1973, Stern 1975) or horizontal convection that occurs when the fluid is differentially heated on a level surface (compare Stern 1975). As a further simplification these studies suppose the density to vary linearly with temperature. To study sinking plumes, the density dependence on temperature has to be approximated at at least quadratic and the simplest case will therfore be a mixture of the above mentioned cases. That makes the use of numerical models nearly unavoidable.

A two-dimensional numerical study of convective flow in an ice-covered lake was done by Svensson( ). Only a few studies have been conducted solely on sinking plumes. Pena et al.(1975) employed an integral approach, assuming similarity in velocity and temperature profile, to compute a round warm water jet, as well as a slot jet, discharging into stagnant water at freezing temperatures.

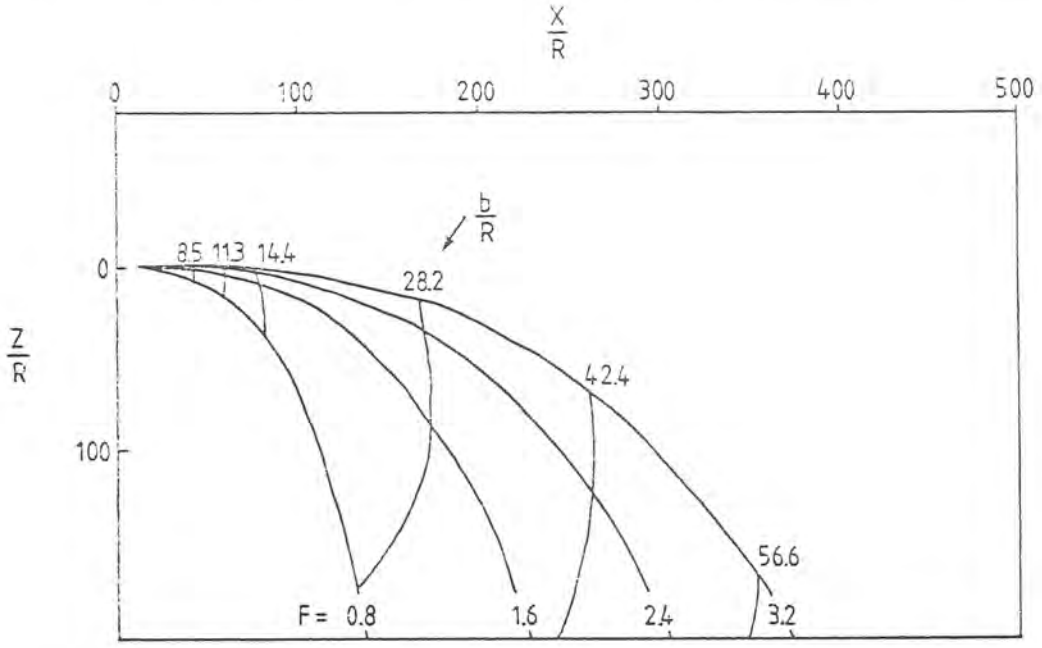

Figure 5 Centerline trajectory and half-width of round jets.

$F = \frac{\mu_0}{\sqrt{gR}}$, ΔT = 11 C, R = initial radius,

b = width

Fig 5 shows results typically obtained from such a model. Besides some assumptions used in this model being questionable (compare Mehrotra 1976), the model does not give any information on how the warm water spreads on the bottom. A much more advanced three-dimensional numerical model, which will be discussed later, was developed by Raithby (1976). At SMHI a two-dimensional model developed by Wilmot (1976) was applied to the

sinking plume problem, first in order to show that such a model is able to reproduce "sinking", later to test how sensitive the physical process is to different assumptions, expecially to a change in size of the vertical and horizontal turbulent eddy coefficients.

MATHEMATICAL FORMULATION AND VARIOUS APPROXIMATIONS

Basically the fundamental hydrodynamic equations imply the existence of convective motions (compare Thompson 1967). Assuming that heating due to compression or cooling due to expansion is neglected, that heat sources enter as boundary condition and neglecting Coriolis forces due to the small spatial scale of the plume, the equations discribing a compresible fluid are

$$\operatorname{div} \vec{v} = -\frac{1}{\rho}\frac{d\rho}{dt} \qquad \text{continuity equation}$$

$$\rho \frac{du}{dt} = -\frac{\partial p}{\partial x} + \frac{1}{3}\mu \frac{\partial}{\partial x} \operatorname{div} \vec{v} + \mu \Delta u$$

$$\rho \frac{dv}{dt} = -\frac{\partial p}{\partial y} + \frac{1}{3}\mu \frac{\partial}{\partial y} \operatorname{div} \vec{v} + \mu \Delta v \qquad \text{momentum (Navier Stokes) equations}$$

$$\rho \frac{dw}{dt} = -\frac{\partial p}{\partial z} + \rho g + \frac{1}{3}\mu \frac{\partial}{\partial z} \operatorname{div} \vec{v}\ \mu \Delta w$$

$$\frac{d(\rho C_p T)}{dt} = k \Delta T \qquad \text{heat equation}$$

$$\rho = \rho\,(p,T,S) \qquad \text{equation of state}$$

$$S = \text{const.}$$

In winter cinditions, the salinity in the area under consideration can be assumed to be constant as a first approximation. It is, however, no fundamental difficulty to allow for variable salinity.

Density appears in the momentum equation in the inertia term (first term) and in the bouyancy term. Rewriting the friction term

$$\frac{1}{3}\mu \operatorname{grad} \operatorname{div} \vec{v} + \mu \Delta \vec{v} = \frac{4}{3}\mu \operatorname{grad} \operatorname{div} \vec{v} - \mu \operatorname{curl} \operatorname{curl} \vec{v}$$

there are frictional effects due to rotation (second

term) and (through the continuity equation) due to changes in density (first term). This term will vanish if a particle following the fluid motion retains its density, that is $\frac{d\rho}{dt} = 0$. This is stronger than assuming incompressibility, i.e. $\frac{\partial \rho}{\partial p} = 0$, (compare Krauss 1973) as,

$$\frac{d}{dt} = \frac{\partial p}{\partial \rho}_{S,T} \frac{d\rho}{dt} + \frac{\partial \rho}{\partial S}_{p,T} \frac{dS}{dt} + \frac{\partial \rho}{\partial T}_{S,p} \frac{dT}{dt} = 0$$

That also simplifies the continuity equation to div $\vec{v}$ = 0 and the heat equation to $\frac{dT}{dt} = \frac{k}{\rho Cp} \Delta T$

if Cp is constant.

Letting p and ρ vary around the values p_0 and ρ_0 in a reference state of hydrostatic equilibrium for which $\frac{\partial p}{\partial z} = \rho_0 g$ and rewriting the momentum equations yields

$$\left(1 + \frac{\rho-\rho_0}{\rho_0} \right) \frac{du}{dt} = - \frac{1}{\rho_0} \frac{\partial (p-p_0)}{\partial x} + \mu \Delta u$$

for v respektively

$$\left(1 + \frac{\rho-\rho_0}{\rho_0} \right) \frac{dw}{dt} = - \frac{1}{\rho_0} \frac{\partial (p-p_0)}{\partial x} + \frac{\rho-\rho_0}{\rho_0} g + \mu \Delta w$$

As $\frac{\rho-\rho_0}{\rho_0}$ is small -variation in temperature over 10 °C change the density at most 1 % - it produces only a small correction to the inertia term but is of primary importance in the buoyancy term (compare Turner 1973). Neglecting $\frac{\rho-\rho_0}{\rho_0}$ in the inertia term is the so called Boussinesq approximation. Phillips (1966) showed that it is also valid when treating convection problems.

Convective motion can be liminar or turbulent. In a sinking plume thereis, of course, shear induced turbulence occuring at a critical Reynold´s number. In addition, convective motion caused entirely by density

differences, where a Reynold´s number does not exist, becomes turbulent under critical conditions. For this kind of motion the change from laminar to turbulent convection is determined by a critical Grashof number (Landau, Lifschitz 1975), that is by the ratio of Rayleigh number (see p. 4) and Prandl number.

To introduce turbulence into the equation of motion and the heat equation it is commonly assumed that there exists a clear deviation between small-scale and large-scale motion, defining

$$F = \bar{F} + F' \text{ with } \bar{F} = \frac{1}{2t_0} \int_{t-t_0}^{t+t_0} F(\tau)d\tau \text{ and } \bar{F'} = 0$$

This assumption is somewhat doubtfull, for instance, when treating thermal convection in a fluid at rest. There are more satisfying ways of averaging (see, for example, Monin 1971) but in the practical application they mostly come down to the above assumption.

With $\P = p - p_0$ and $\nu = \frac{\mu}{\rho_0}$

$$\operatorname{div} \vec{v} = 0$$

$$\frac{d\bar{u}}{dt} = -\frac{1}{\rho_0}\frac{\partial \bar{\P}}{\partial x} + \frac{\partial}{\partial x}(\nu\frac{\partial \bar{u}}{\partial x} - \overline{u'^2}) + \frac{\partial}{\partial y}(\nu\frac{\partial \bar{u}}{\partial y} - \overline{v'u'}) + \frac{\partial}{\partial z}(\nu\frac{\partial \bar{u}}{\partial z} + \overline{w'u'})$$

for $\bar{v}$ respectively

$$\frac{d\bar{w}}{dt} = -\frac{1}{\rho_0}\frac{\partial \P}{\partial z} + \frac{(\rho-\rho_0)}{\rho_0} g + \frac{\partial}{\partial x}(\nu\frac{\partial \bar{w}}{\partial x} + \overline{u'w'}) +$$

$$\frac{\partial}{\partial y}(\nu\frac{\partial \bar{w}}{\partial y} + \overline{v'w'}) + \frac{\partial}{\partial z}(\nu\frac{\partial \bar{w}}{\partial z} + \overline{w'^2})$$

$$\frac{d\bar{T}}{dt} = \frac{\partial}{\partial x}\left(\frac{k}{Cp\rho_0}\frac{\partial \bar{T}}{\partial x} - \overline{u'T'}\right) + \frac{\partial}{\partial y}\left(\frac{k}{Cp\rho_0}\frac{\partial T}{\partial y} - \overline{v'T'}\right) +$$

$$\frac{\partial}{\partial z}\left(\frac{k}{Cp\rho_0}\frac{\partial \bar{T}}{\partial z} + \overline{w'T'}\right)$$

In the following the overbar is dropped again.

MODEL EQUATIONS

In order to do some basic numerical studies the above equations are further simplified and horizontally averaged. The Reynold stresses and the turbulent heat exchange are modelled using eddy viscosities and turbulent heat conduction coefficients. Averaging horizontally as $\bar{F} = \frac{1}{b}\int_0^b F(\beta)d\beta$ and dropping the overbar yields for b = const and $\rho = (1 + \sigma_t\, 10^{-3})$ g/cm^3, $\rho_0 = 1$ g/cm^3 :

$$\frac{du}{dt} = -\frac{\partial \P}{\partial x} + (A_h + \nu)\frac{\partial^2 u}{\partial x^2} + \frac{\partial}{\partial z}\left(\left[A_v + \nu\right]\frac{\partial u}{\partial z}\right)$$

$$\frac{dw}{dt} = -\frac{\partial \P}{\partial z} + g\sigma_t 10^{-3} + (A_h + \nu)\frac{\partial^2 w}{\partial x^2} + \frac{\partial}{\partial z}\left(\left[A_v + \nu\right]\frac{\partial w}{\partial z}\right)$$

$$\frac{dT}{dt} = (K_h + \kappa)\frac{\partial^2 T}{\partial x^2} + \frac{\partial}{\partial z}\left(\left[K_v + \kappa\right]\frac{\partial T}{\partial z}\right)$$

$$0 = \frac{\partial u}{\partial x} + \frac{\partial w}{\partial z}$$

where the horizontal eddy coefficients are assumed to be constant whereas the vertical eddy coefficients are allowed to be a spatial variable.

Cross differentation and subtraction of the momentum equations gives an equation for the vorticity component, $\eta = -\frac{\partial u}{\partial z} + \frac{\partial w}{\partial x}$, perpendicular to the vertical plane and eliminates the pressure from the momentum equations.

$$\frac{d\eta}{dt} = 10^{-3} g \frac{\partial \sigma_t}{\partial x} + (A_h + \nu)\frac{\partial^2 \eta}{\partial x^2} + \frac{\partial}{\partial z}\left(\left[A_v + \nu\right]\frac{\partial \eta}{\partial z}\right) +$$

$$\frac{\partial}{\partial z}\left[\frac{\partial A_v}{\partial x}\frac{\partial w}{\partial z} - \frac{\partial A_v}{\partial z}\frac{\partial u}{\partial z}\right]$$

Comparing the last two terms

$$\frac{\partial}{\partial z}\left(A_v \frac{\partial \eta}{\partial z}\right) = -\frac{\partial A_v}{\partial z}\frac{\partial^2 u}{\partial z^2} + \frac{\partial A_v}{\partial z}\frac{\partial^2 w}{\partial z \partial x} - A_v \frac{\partial^2 u}{\partial z^2} + A_v \frac{\partial^2 w}{\partial z \partial x} \text{ and}$$

$$\frac{\partial}{\partial z}\left(\frac{\partial A_v}{\partial x}\frac{\partial w}{\partial z} - \frac{\partial A_v}{\partial z}\frac{\partial u}{\partial z}\right) = -\frac{\partial A_v}{\partial z}\frac{\partial^2 u}{\partial z^2} + \frac{\partial^2 A_v}{\partial z \partial x}\frac{\partial w}{\partial z} -$$

$$\frac{\partial^2 A_v}{\partial z^2}\frac{\partial u}{\partial z} + \frac{\partial A_v}{\partial x}\frac{\partial^2 w}{\partial z^2}$$

shows that although the first two terms on the right hand side are of the same order of magnitude, the predominent terms of the first equation (term 3 and 4) are an order of magnitude bigger than the corresponding terms of the second equation. Therefore the last term of the vorticity equation is neglected what in fact means that vorticity is diffused in the same way as momentum.

Defining a transport -stream function by $u = -\frac{1}{b}\frac{\partial \psi}{\partial z}$ and $w = \frac{1}{b}\frac{\partial \psi}{\partial x}$, $\eta = -\frac{\partial u}{\partial z} + \frac{\partial w}{\partial x}$, is recast as an elliptic Poisson equation $\eta = \frac{1}{b}\left(\frac{\partial^2 \psi}{\partial z^2} + \frac{\partial^2 \psi}{\partial x^2}\right)$ and u and w can be determinded from the above equations for ψ.

The above equations are normalized by the advective time scale $t_0 = L/U_0$, where L is a characteristic length and U_0 a characteristic horizontal advection velocity. Defining the nondimensional quantities $t'=t/t_0$, $x'=x/L$, $z'=z/L$, $u'=u/U_0$, $w'=w/U_0$, $\eta'=\eta \cdot t_0$, $T'=T/T_0$, $U_0=L/t_0$ and $VMIX=K_v/K_{v\ SCALE}$ and dropping the prime, yeilds:

$$\frac{\partial T}{\partial t} = \varepsilon \delta_k \left(1 + \frac{\kappa}{K_h}\right)\frac{\partial^2 T}{\partial x^2} + \varepsilon \frac{\partial}{\partial z}\left(\left[VMIX + \frac{\kappa}{K_v}\right]\frac{\partial T}{\partial z}\right)$$

where $\varepsilon = \frac{K_v t_0}{L^2}$ and $\delta_k = \frac{K_h}{K_v}$, $\frac{\partial u}{\partial x} + \frac{\partial w}{\partial z} = 0$ and

$$\frac{\partial \eta}{\partial t} = Fr^{-2} 10^{-3} \frac{\partial \sigma_t}{\partial x} + Pr\varepsilon\delta_A \left(1 + \frac{\nu}{A_h}\right) \frac{\partial^2 \eta}{\partial x^2} +$$

$$Pr\varepsilon \frac{\partial}{\partial z} \left(\left[VMIX + \frac{\kappa}{A_v} \right] \frac{\partial \eta}{\partial z} \right)$$

where $Pr = A_v/K_v$, $\delta_A = A_h/A_v$ and $Fr = \frac{U_0}{\sqrt{gL}}$ the Froude number.

The last equation is rather illuminating, considering that in a barotropic flow vorticity is only created at rigid walls and from there diffused into the flow. Disregarding this effect by assuming slip walls, the vorticity remains constant in a barotropic flow, whereas in a baroclinic flow horizontal density differences drive the motion. The following picture is supposed to demonstrate what positive or negative vorticity can mean in terms of velocity profiles.

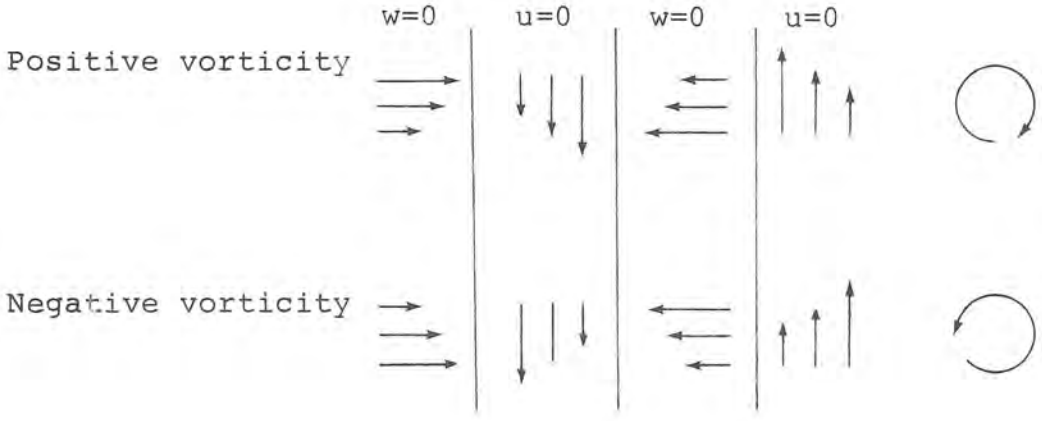

That is: positive vorticity followed horizontally by negative vorticity indicates a zone of convergence or, in other words: sinking.

As the horizontal temperature gradient in a surface plume is predominately negative, the dependence of density on temperature has to be nonlinear to allow the

vorticity to change sign. Using the accurate relations defining σ_t (Knudsen's Hydrographical Tables, 1901) is very time consuming. An approximation developed for high salinities (Friedrich et al. 1972) and modified for low salinities (Wilmot 1976) gives still a poor fit for low temperatures. (See fig 6). Therefore, the accurate σ_t-curve for a particular salinity is fitted by a parabel which yields (see fig 6).

$\sigma_t = -8\ 10^{-3}\ (T - 2.5)^2 + 5.8$ for $S = 7.2$ ‰ .

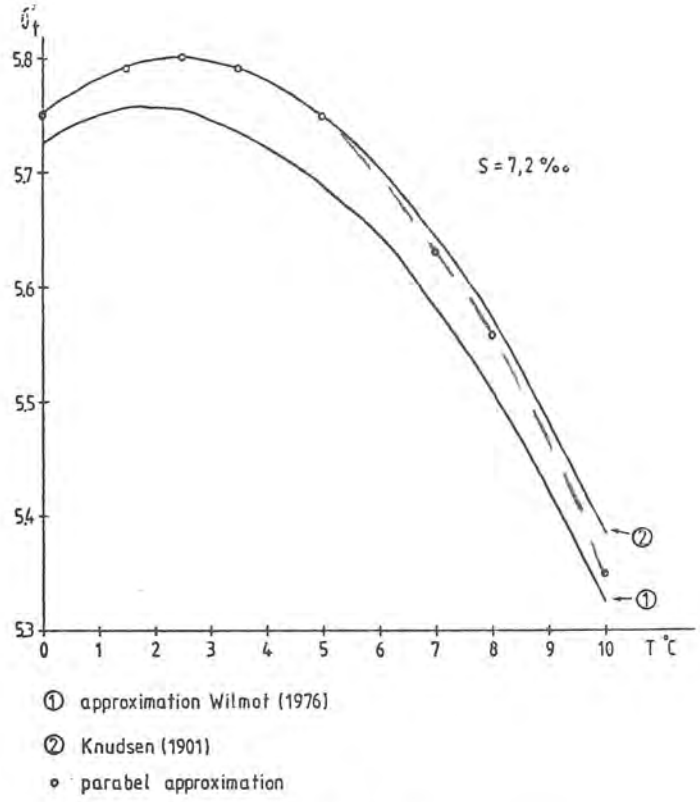

Figure 6. Different approximations for the dependence of density on temperature.

With $\frac{\partial \sigma_t}{\partial x} = -\ 0.016\ (T - 2.5)\ \frac{\partial T}{\partial x}$ and a negative horizontal temperature gradient, the source term in the vorticity equation becomes negative for T less than 2.5 which is the temperature of maximum density.

The nondimensional equation for vorticity shows that the

importance of the source term decreases with increasing Froude number or with increasing horizontal advection velocity (compare fig 5). Increasing horizontal mixing has the same effect, as it yields a fast diminishing of the horizontal density gradient. Sinking plumes are, for instance not observed if there are strong winds.

MODEL BOUNDARY CONDITIONS

In a barotropic case the vorticity equation determines how vorticity is transported, but the total vorticity is conserved in the interior. What actually drives the circulation is the vorticity produced at rigid walls and the wind induced vorticity at the surface. When modelling a sinking plume, however, horizontal density differences are the major driving mechanisms. Therefore, a simple slip wall condition at rigid walls is modelled. That is $\frac{\partial u}{\partial z} = 0$ at a horizontal wall and $\frac{\partial w}{\partial x} = 0$ at a vertical wall. Remembering that a rigid wall must be a streamline, i.e. $\Psi w = \text{const.} = 0$, yields $\eta = 0$. Using a slip condition has the further advantage that difficulties arising in modelling vorticity at sharp convex corners (Roache 1972) are avoided.

For simplicity, the wind stress at the surface is assumed to be zero. Free surface variations in the plume are on the order of a few millimeters. The slope of the free surface is, however, directly related to local pressure gradients that generate the dispersion of the flow (Policastro et al. 1975). Therefore, the free-surface location must be calculated with good accuracy. Yet, for the sake of simplicity (being able to use a fixed grid) and efficiency (bigger time step) of the numerical procedure, a rigid lid approximation is used, fixing $\psi_{surface} = \text{const.}$ at $z = 0$ and thereby $w\ (z=0) = 0$.

At open vertical boundaries a zero horizontal gradient of vorticity is assumed as well as $\frac{\partial w}{\partial x} = 0$. The ψ-value at that boundary is then determined from $\eta = \frac{1}{b} \frac{\partial^2 \psi}{\partial z^2}$, i.e. from the equation that defines vorticity if $\frac{\partial w}{\partial x}$ is zero (Roache 1972).

The boundary conditions for temperature are those described in Wilmot (1976):

$K_v \frac{\partial T}{\partial z} - wT = 0$ at horizontal rigid walls

$-K_h \frac{\partial T}{\partial x} + uT = 0$ at upstreams vertical rigid walls

As u_{wall} is zero, at a vertical rigid wall, $\frac{\partial T}{\partial x} = 0$ is sufficient to model the last condition, although $K_h \frac{\partial T}{\partial x}$ is zero because K_h is zero at the wall.

$-K_v \frac{\partial T}{\partial z} + wT = - Q_{\Delta T}$ at the surface

$Q_{\Delta T}$ is the net heat loss due to the overtemperature. As seen from table 1 $Q_{\Delta T} / \Delta T$, where T is the overtemperature, is rather constant for constant wind conditions when computed from the equations quoted by Wilmot (1976). Therefore, it is modeled by a constant coefficient. Most of the numerical experiments, however, were preformed by assuming $Q_{\Delta T}$ to be zero.

TABLE 1

Net heat loss due to overtemperature divided by the overtemperature ΔT, assuming an ambient temperature $T_a = 0$.

$Q_{\Delta T} = \frac{\partial Q \Delta T}{\partial T} \Delta T$

table gives $\frac{\partial Q \Delta T}{\partial T} 10^3$ in cal cm^{-2} sec^{-1} $degree^{-1}$

wind velocity / ΔT	0 m/sec	1 m/sec	5 m/sec
10 °C	0.36	0.50	1.33
1 °C	0.28	0.39	1.06
0.1 °C	0.28	0.38	1.05

At open vertical boundaries T is prescribed if there is a flow into the interior whereas $\frac{\partial T}{\partial x}$ is zero if the fluid leaves the area under consideration.

NUMERICAL MODEL

For the integration of the vorticity and temperature equation, a numerical model developed by Wilmot (1976) is applied, making use of a later extension to a semi-implicit scheme for vertical diffusion (Wilmot 1977), which yields the following time structure

$$\frac{1}{2\Delta t}\left(F^{n+1} - F^{n-1}\right) = (\text{source fo } F)^{n} - (\text{advection of } F)^{n} + (\text{horizontal diffusion of } F)^{n-1} + 1/2\ (\text{vertical diffusion of } F)^{n-1} + 1/2\ (\text{vertical diffusion of } F)^{n+1}$$

In order to avoid a splitting of the solution at adjacent time levels, which is inherent to the leapfrog scheme used by the model, smoothing occurs at regular time intervals.

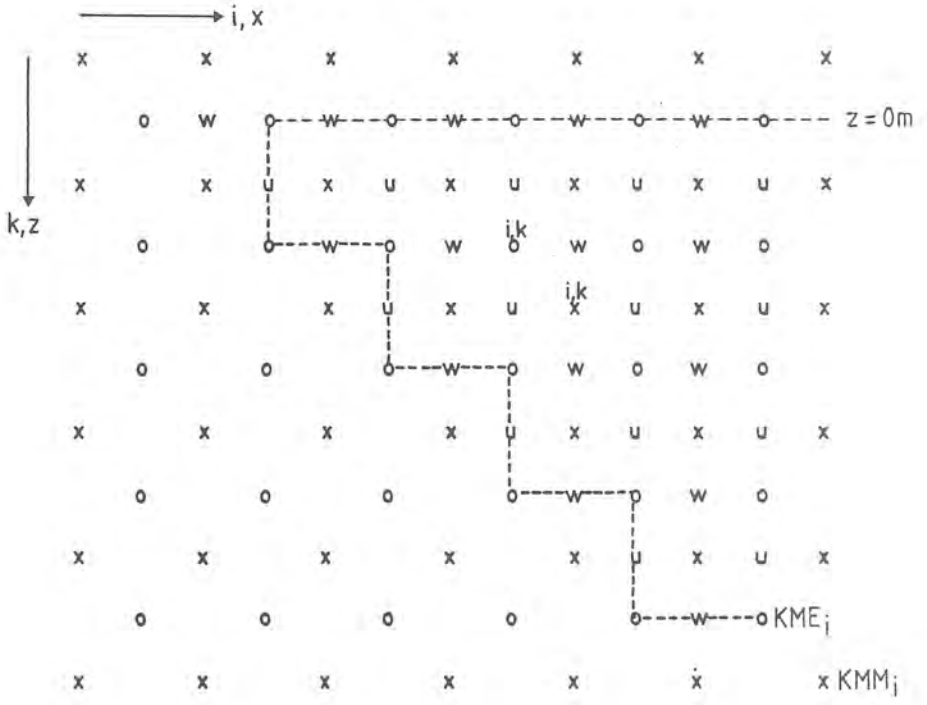

------ boundary
o = streamfunction and vorticity grid point
x = temperature and VMIX point

Figure 7

Using the staggered grid (fig 7) and the difference form for advection (the Arakawa flux form) and for diffusion, described by Wilmot (1976), results in the following equations for vorticity and temperature in a channel with constant width:

$$- Pr\varepsilon \frac{2\Delta t}{4\Delta z^2} (VMIX^n_{i+1,K} + VMIX^n_{i,K} + \frac{2\nu}{A_v}) \eta^{n+1}_{i,K-1}$$

$$+ \left[1 + Pr\varepsilon \frac{2\Delta t}{4\Delta z^2} (VMIX^n_{i+1,K} + VMIX^n_{i,K} + \frac{2\nu}{A_v} + VMIX^n_{i+1,K+1} + VMIX^n_{i,K+1} + \frac{2\nu}{A_v}) \right] \eta^{n+1}_{i,K}$$

$$- Pr\varepsilon \frac{2\Delta t}{4\Delta z^2} (VMIX^n_{i+1,K+1} + VMIX^n_{i,K+1} + \frac{2\nu}{A_v}) \eta^{n+1}_{i,K+1}$$

$$= \eta^{n-1}_{i,K}$$

$$+ Fr^{-2} \frac{2\Delta t}{2\Delta x} (\sigma^n_{i,K} + \sigma^n_{i,K+1} - \sigma^n_{i+1,K} - \sigma^n_{i+1,K+1})$$

$$- \frac{2\Delta t}{4\Delta x \Delta z} \frac{1}{b} \left[\eta^n_{i+1,K} (-\psi^n_{i+1,K+1} + \psi^n_{i+1,K-1}) - \eta^n_{i-1,K} (-\psi^n_{i-1,K+1} + \psi^n_{i-1,K-1}) \right.$$

$$\left. + \eta^n_{i,K+1} (\psi^n_{i+1,K+1} - \psi^n_{i-1,K+1}) - \eta^n_{i+1,K} (\psi^n_{i+1,K-1} - \psi_{i-1,K-1}) \right]$$

$$+ Pr\varepsilon\delta_A (1 + \frac{\nu}{A_h}) \frac{2\Delta t}{\Delta x^2} (\eta^{n-1}_{i+1,K} - 2\eta^{n-1}_{i,K} + \eta^{n-1}_{i-1,K})$$

$$+ Pr\varepsilon \frac{2\Delta t}{4\Delta z^2} \left[(VMIX^n_{i+1,K+1} + VMIX^n_{i,K+1} + \frac{2\nu}{A_v}) (\eta^{n-1}_{i,K+1} - \eta^{n-1}_{i,K}) \right.$$

$$- \left(VMIX^{n}_{i+1,K} + VMIX^{n}_{i,K} + \frac{2\nu}{A_v}\right)\left(\eta^{n-1}_{i,K} - \eta^{n-1}_{i,K-1}\right)\Bigg]$$

At each timestep this leads to a set of algebraic equations,

$\eta_{i,1}$ = surface boundary condition

$\alpha_2\eta_{i,1} + \beta_2\eta_{i,2} + \gamma_2\eta_{i,3}$ = $ERHS_2$

$\alpha_K\eta_{i,K-1} + \beta_K\eta_{i,K} + \gamma_K\eta_{i,K+1}$ = $EHRS_K$

$\alpha_{KME-1}\eta_{i,KME-2}\beta_{KME-1}\eta_{i,KME-1} + \gamma_{KME-1}\eta_{i,KME}$ = $ERHS_{KME-1}$

$\eta_{i,KME}$ = bottom boundary condition

which are solved by simple Gaussion elimination.

The temperature equation takes the form:

$$-\varepsilon \frac{2\Delta t}{4\Delta z^2}\left(VMIX^{n}_{i,K} + VMIX^{n}_{i,K-1} + \frac{2\kappa}{K_v}\right) T^{n+1}_{i,K-1}$$

$$+\left[1 + \varepsilon \frac{2\Delta t}{4\Delta z^2}\left(VMIX^{n}_{i,K} + VMIX^{n}_{i,K-1} + \frac{2\kappa}{K_v} + VMIX^{n}_{i,K+1} + VMIX^{n}_{i,K} + \frac{2\kappa}{K_v}\right)\right] T^{n+1}_{i,K}$$

$$-\varepsilon \frac{2\Delta t}{4\Delta z^2}\left(VMIX^{n}_{i,K+1} + VMIX^{n}_{i,K} + \frac{2\kappa}{K_v}\right) T^{n+1}_{i,K+1}$$

$$= T^{n-1}_{i,K}$$

$$- \frac{2\Delta t}{2\Delta x\Delta z}\frac{1}{b}\left(-\psi^n_{i,K} + \psi^n_{i,K-1}\right)\left(T^n_{i+1,K} + T^n_{i,K}\right) \qquad +XFLUXP$$

$$+ \frac{2\Delta t}{2\Delta x\Delta z}\frac{1}{b}\left(-\psi^n_{i-1,K} + \psi^n_{i-1,K-1}\right)\left(T^n_{i,K} + T^n_{i-1,K}\right)$$

$$- \frac{2\Delta t}{2\Delta x\Delta z}\frac{1}{b}\left(\psi^n_{i,K} - \psi^n_{i-1,K}\right)\left(T^n_{i,K+1} + T^n_{i,K}\right) \qquad +ZFLUXP$$

$$+ \frac{2\Delta t}{2\Delta x\Delta z}\frac{1}{b}\left(\psi^n_{i,K-1} - \psi^n_{i-1,K-1}\right)\left(T^n_{i,K} + T^n_{i,K-1}\right)$$

$$+\varepsilon\delta_K\left(1+\frac{\kappa}{K_h}\right)\frac{2\Delta t}{\Delta x^2}\left(T^{n-1}_{i+1,K} - T^{n-1}_{i,K}\right)$$

$$-\varepsilon\delta_K\left(1+\frac{\kappa}{K_h}\right)\frac{2\Delta t}{\Delta x^2}\left(T^{n-1}_{i,K} - T^{n-1}_{i-1,K}\right) \qquad -XFLUXM$$

$$+\varepsilon\frac{2\Delta t}{4\Delta z^2}\left(VMIX^n_{i,K+1} + VMIX^n_{i,K} + \frac{2\kappa}{K_v}\right)\left(T^{n-1}_{i,K+1} - T^{n-1}_{i,K}\right)$$

$$-\varepsilon\frac{2\Delta t}{4\Delta z^2}\left(VMIX^n_{i,K} + VMIX^n_{i,K-1} + \frac{2\kappa}{K_v}\right)\left(T^{n-1}_{i,K} - T^{n-1}_{i,K-1}\right) \qquad -ZFLUXM$$

and the resulting set of algebraic equations is:

$$\beta_1 T_{i2} + \gamma_1 T_{i3} = TRHS_1 \quad \text{(including boundary condition } ZFLUXM = Q\Delta T\,\frac{2\Delta T}{\Delta z}\text{)}$$

$$\alpha_{K-1}\,T_{i,K-1} + \beta_{K-1}\,T_{i,K} + \gamma_{K-1}\,T_{i,K+1} = TRHS_K$$

$$\alpha_{KMM-2} + T_{i,KMM-2} + \beta_{KMM-2}\,T_{i,KMM-1} = TRHS_{KMM-1}$$

(including boundary conditions $ZFLUXP = 0$)

That is, an explicit calculation of $T_{i,1}$ and T_{iKMM} is not needed but fluxes through the boundaries are prescribed.

Using the full third momentum equation necessitates solving a two-dimensional Poisson-equation for the streamfunction. This is done by successive over-relaxation (Roache 1972).

Adding $0 = \psi^{e}_{i,K} - \psi^{e}_{i,K}$ to

$$b\eta^{n+1}_{i,K} = \frac{1}{\Delta z^2}\left(\psi^{e}_{i,K+1} + \psi^{e+1}_{i,K} + \psi^{e+1}_{i,K-1}\right) + \frac{1}{\Delta x^2}\left(\psi^{e}_{i+1,K} + \psi^{e+1}_{i,K} + \psi^{e+1}_{i-1,K}\right)$$

where e is the interation level, and rearranging the equation leads to

$$\psi^{e+1}_{i,K} = \psi^{e}_{i,K} + \frac{1}{2\left(1 \frac{\Delta x^2}{\Delta z^2}\right)}\left[\psi^{e}_{i+1,K} + \psi^{e+1}_{i-1,K} + \frac{\Delta x^2}{\Delta z^2}\psi^{e}_{i,K+1}\right.$$

$$\left. + \frac{\Delta x^2}{\Delta z^2}\psi^{e+1}_{i,K-1} - b\Delta x^2\eta^{n+1}_{i,K} - 2\left(1 + \frac{\Delta x^2}{\Delta z^2}\right)\psi^{e}_{i,K}\right]$$

In the SOR method, the term in brackets is multiplied by a relaxation factor α, where $\alpha \neq 1$. For convergence it is required that $1 \leqslant \alpha < 2$. The optimum value for α is empirically found by running some test cases.

As the numerical scheme is only semi-implicit, there is a maximum time step. The stability criterion is (compare Wilmot 1976) that the maximum time step Δt, must obey the relation

$$CFL < CFL_{critical} \text{ with } CFL = \Delta t \left(\frac{u_{max}}{\Delta x} + \frac{w_{max}}{\Delta z}\right)$$

as constant Δx and Δz are used

$$\text{and } CFL_{critical} = \sqrt{1 - 8\Delta t\left(\frac{A_v}{\Delta z^2} + \frac{A_h}{\Delta x^2}\right)} \approx \sqrt{1 - 8\Delta t \frac{A_h}{\Delta x^2}}$$

As $CFL_{critical}$ has to be real, Δt is limited to

$$\Delta t < \frac{1}{8} \frac{\Delta x^2}{A_h}$$

Using Δx = 50 m and in most of the calculations A_h = 5 m^2/sec, limits Δt to 60 sec. Typical maximum velocities u_{max} = 10 cm/sec, w_{max} = 0.5 cm/sec and Δz = 1m, allowed a timestep of 30 sec.

RESULTS AND DISCUSSION

The first numerical experiment was performed to demonstrate the basically different behaviour of a sinking plume from a floating plume. Prescribing the same barotropic transport (20 m^3/sec and the same constant coefficient describing vertical dispersion ($A_v = K_v = 10$ cm^2/sec)), the density field of a floating plume creates only positiv vorticity. The warm water is transported in the surface layer (fig 8) with velocities much higher than the velocities corresponding to the barotropic condition.

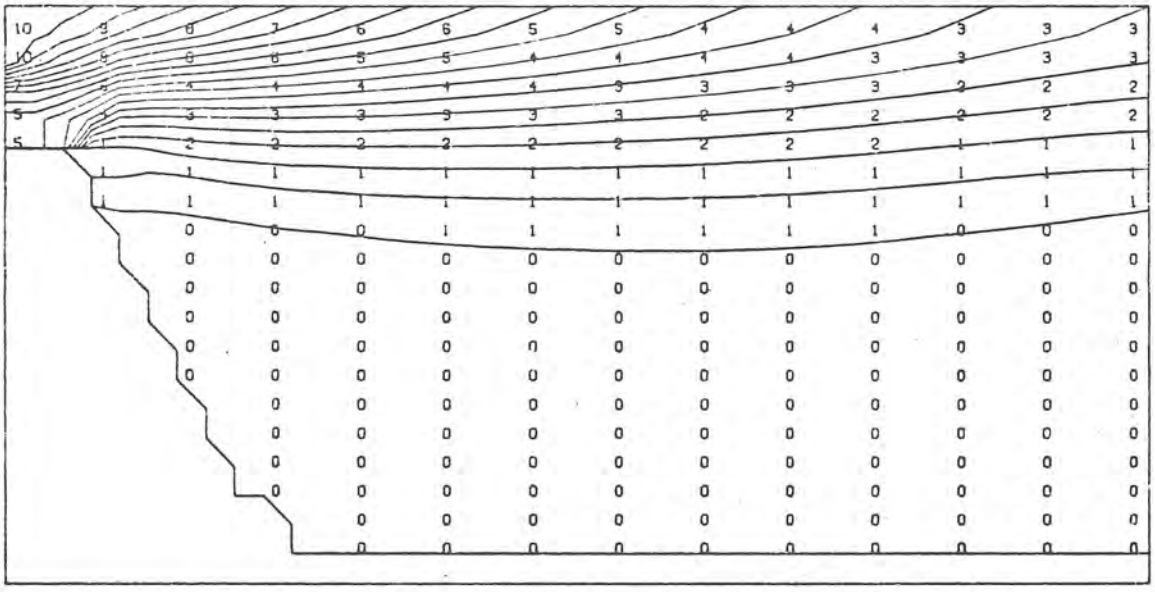

Figur 8. Floating plume ambient temperature 10 °C discharge temperature 20 °C.

This additional out transport is compensated by an in-transport in the bottom layer (fig 9). A downward transport of heat other than by advection due to the barotropic velocity field, is entirely due to vertical mixing.

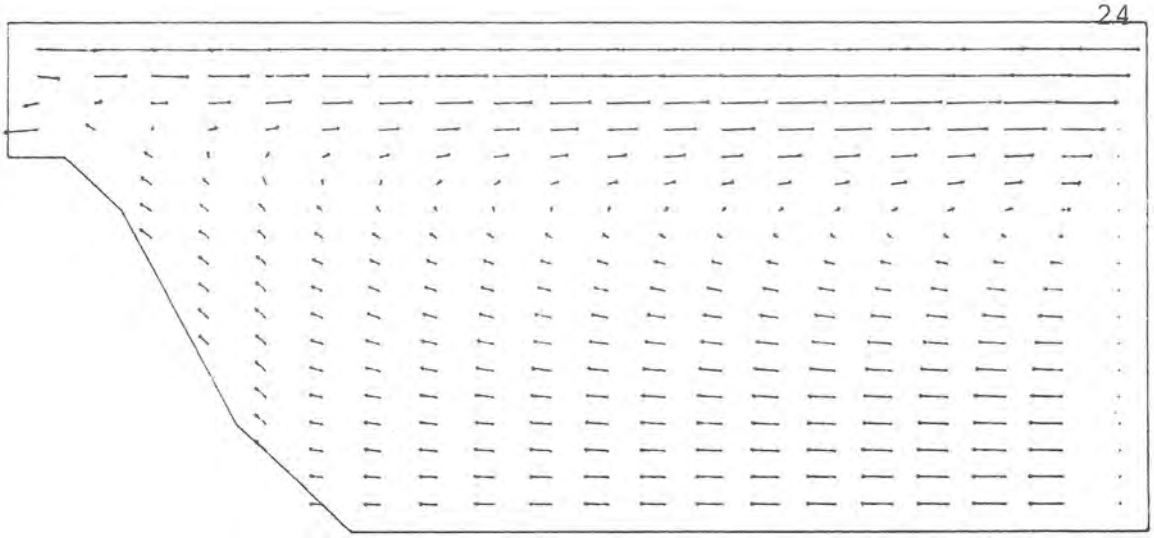

Figure 9. Floating plume, velocity vectors, horizontal scale = 20 x vertical scale.

On the other hand, the feature typical for sinking plumes is a zone of convergence in the front of the plume (fig 10), which becomes more pronounced as the plume developes (fig 11).

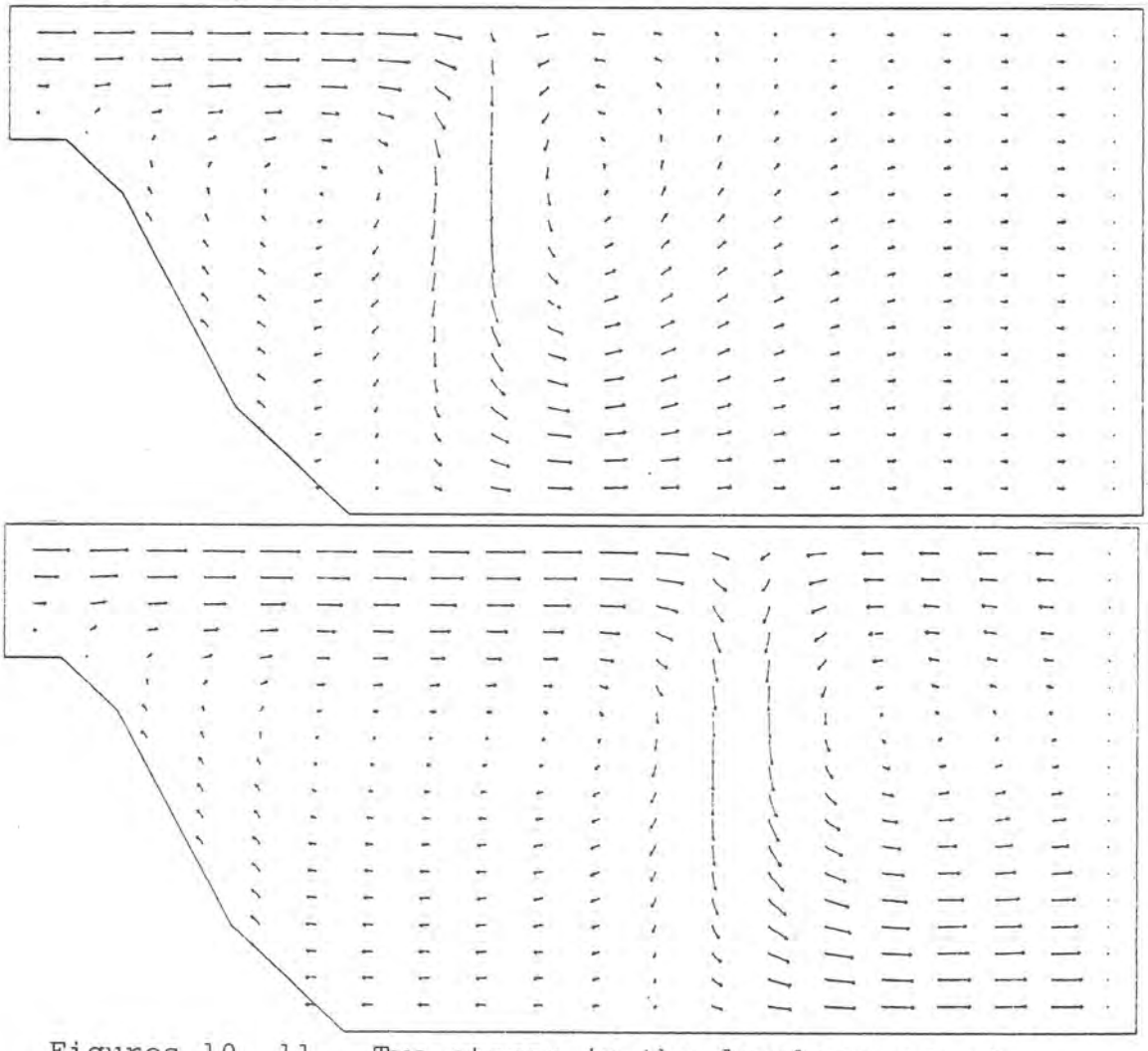

Figures 10, 11. Two stages in the developement of a sinking plume (velocity vectors).

The corresponding isolines indicate the downward transport of heat due to thermal convection (fig 12) and later spreading along the bottom (fig 13). The vertical velocity components in the zone of convergence are in the order of 0.1 to 0.2 cm/sec, increasing slightly with time.

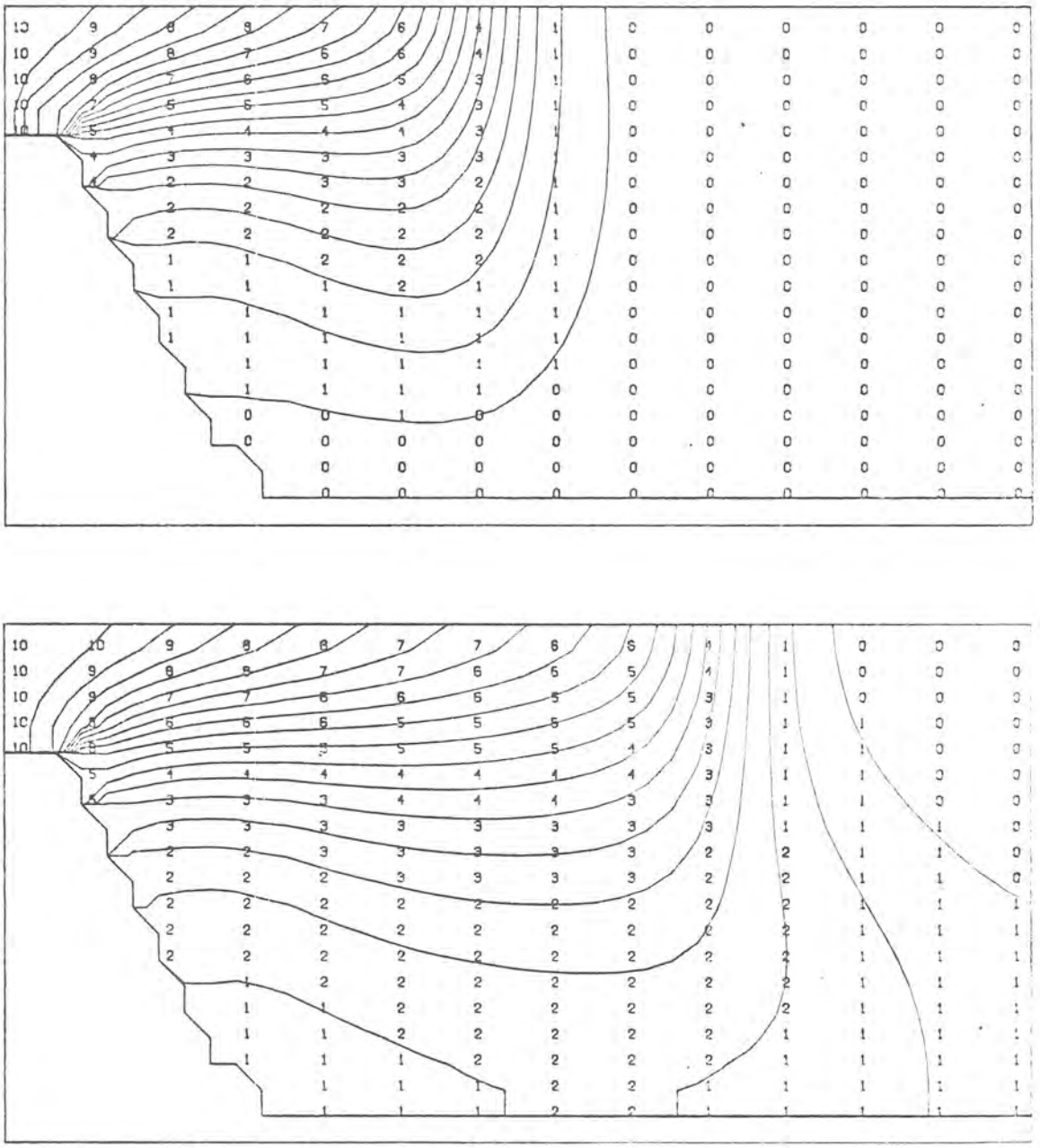

Figures 12, 13. Two stages in the developement of a sinking plume temperature, ambient temperature 0 ^{o}C discharge temperature 10 ^{o}C.

Prescribing only half of the barotropic transport, increases both positive and negative vorticity. The additional vorticity results in an increase of the baroclinic part of the horizontal velocity component both in the surface layer in front of the zone of convergence, and in the bottom layer behind it and causes the total horizontal velocity component, in the vicinity of the zone of convergence, to remain in the same order of magnitude (fig 14), whereas the vertical velocity component decreases by some hundredths cm/sec form W_{max} = 0.18 cm/sec to W_{max} = 0.15 cm/sec.

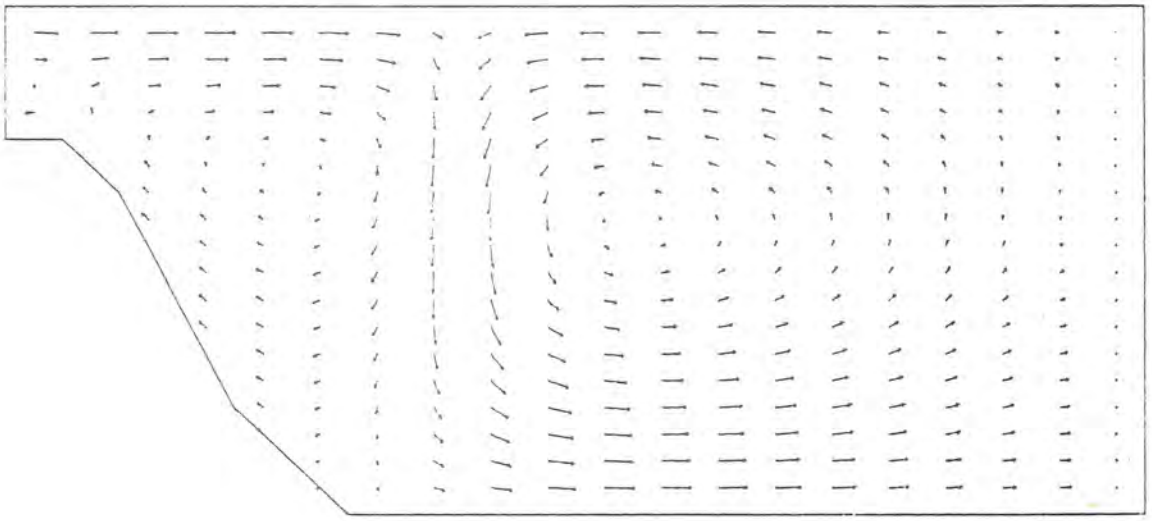

Figure 14. Discharge rate half of that in fig 11/13.

The temperature isolines (fig 15) corresponding to fig 11 show a much shorter plume. Both cases are, however, not run to a steady state, therefore nothing definite can be concluded about the location of the zone of convergence.

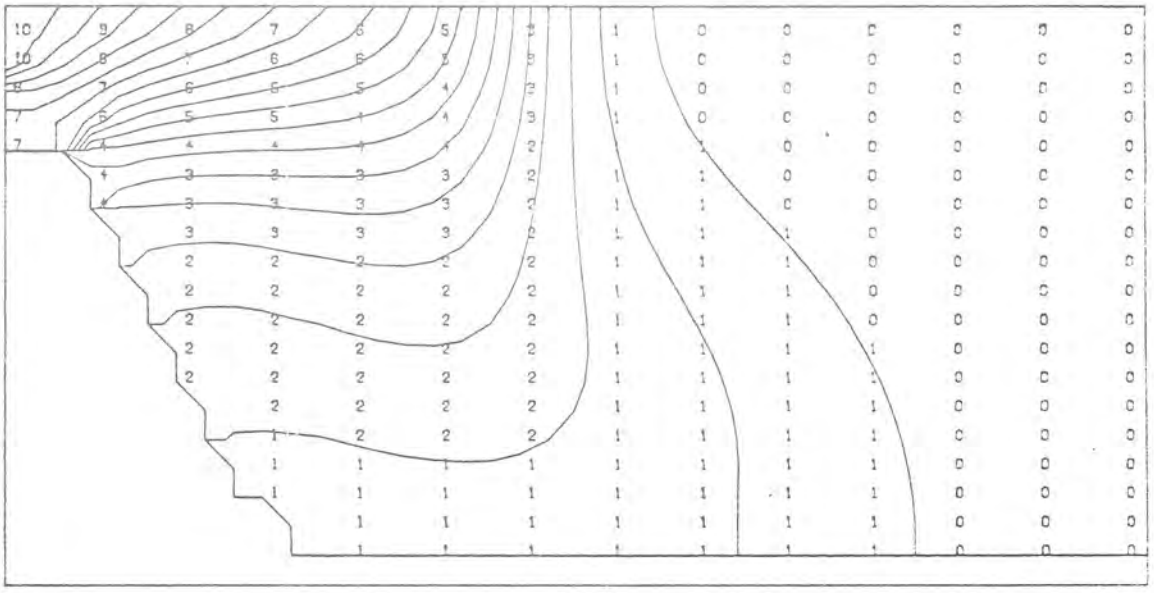

Figure 15. Discharge rate half of that in fig 11/13.

A assumption often made is that the hydrostatic approximation is valid. Comparing figures 14, 15 and figure 16, 17 respectively , this appears to be a good approximation. The diviations in vertical velocity components are only by thousandths cm/sec, the velocities being bigger if the hydrostatic approximation is used.

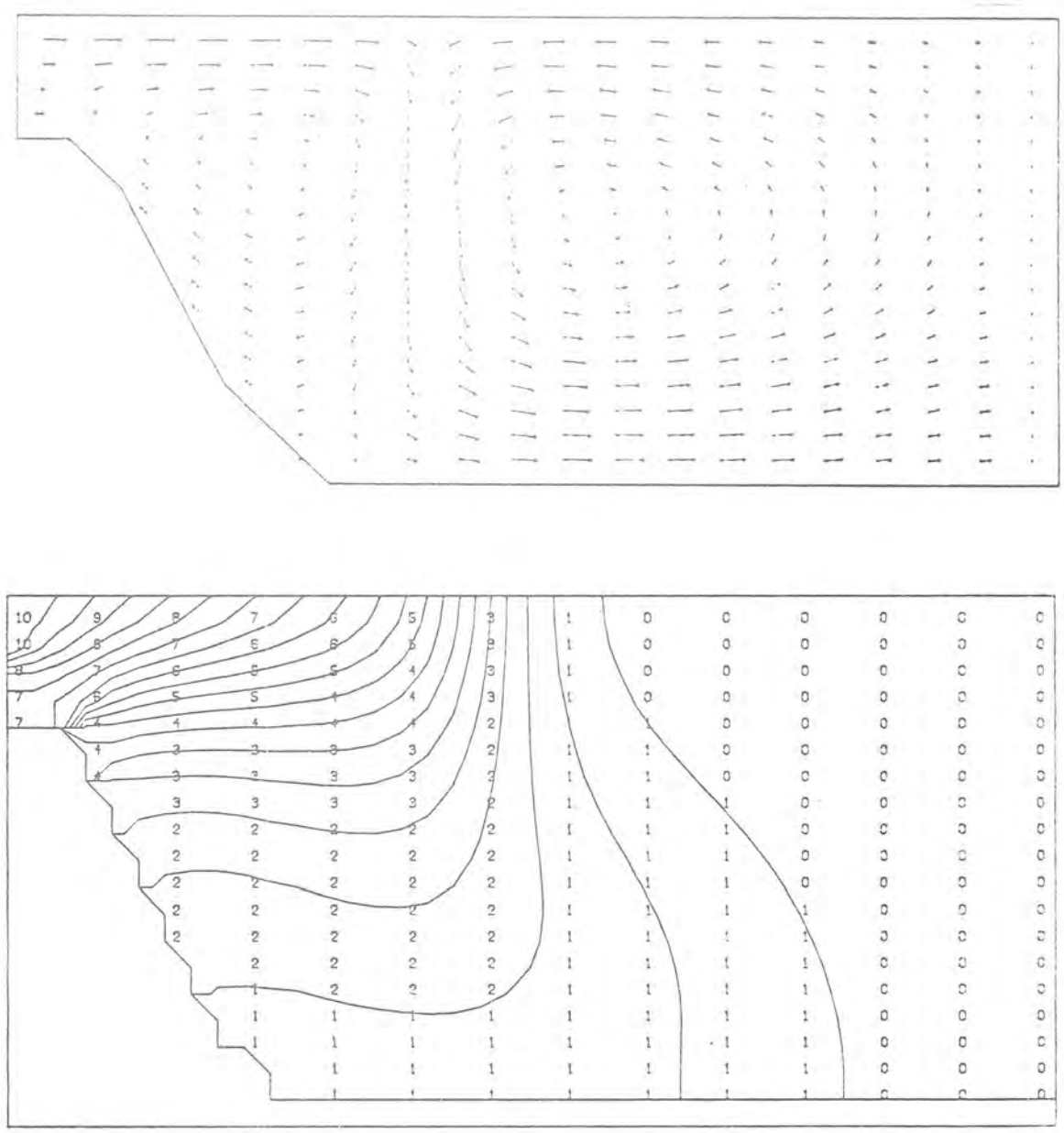

Figures 16, 17. Hydrostatic approximation not used. Compare fig 14, 15.

Pronounced variation on the other hand, can be caused by the bottom topography. When one assumes a hill, instead of a flat bottom, the result of the computation is higher temperature in front of the hill. This is often observed in nature. The high temperatures shown in fig 3 (6 ^{o}C), however, are not explained by the result of this numerical experiment.

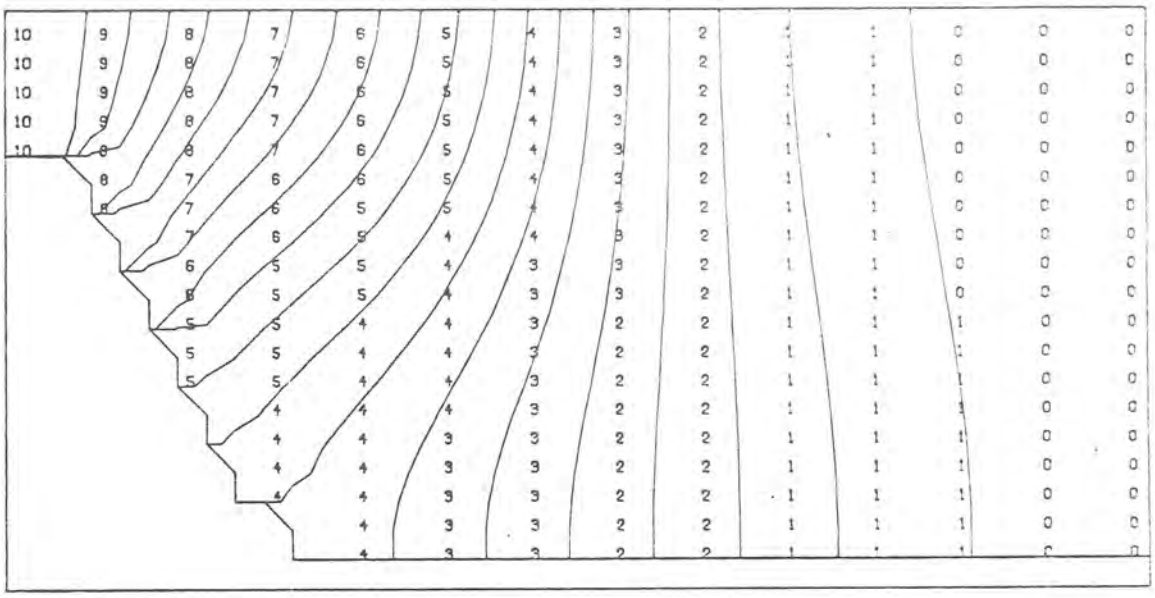

Figure 18. Plume with no heat loss to the atmosphere.

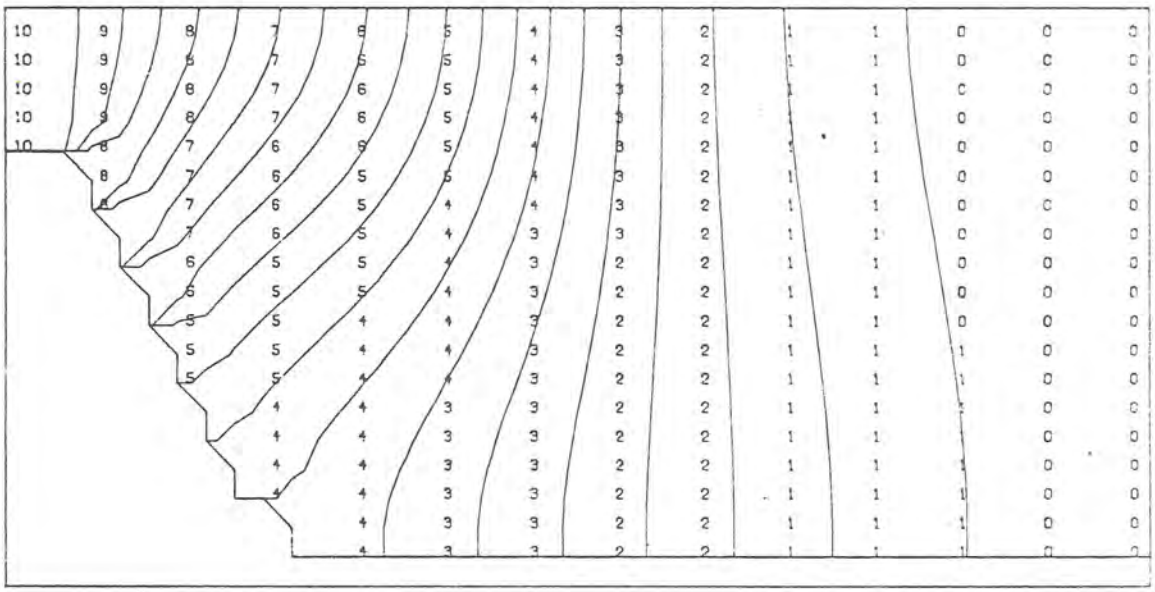

Figure 19. Plume with heat loss to the atmosphere.

All the forgoing experiments were carried out under the assumption that there is no heat loss due to overtemperature at the surface. That is, of course, wrong and was just assumed for convenience. Two corresponding runs with $A_v = K_v = 50$ cm^2/sec and a barotropic transport of 20 m^3/sec show that a rather strong heat loss modelled by $\frac{\partial Q \Delta T}{\partial T} = 10^{-3}$ cal cm^{-2} sec^{-1} degree^{-1} causes

the isolines to steepen and thereby the plume shortens slightly (fig 18), (fig 19).

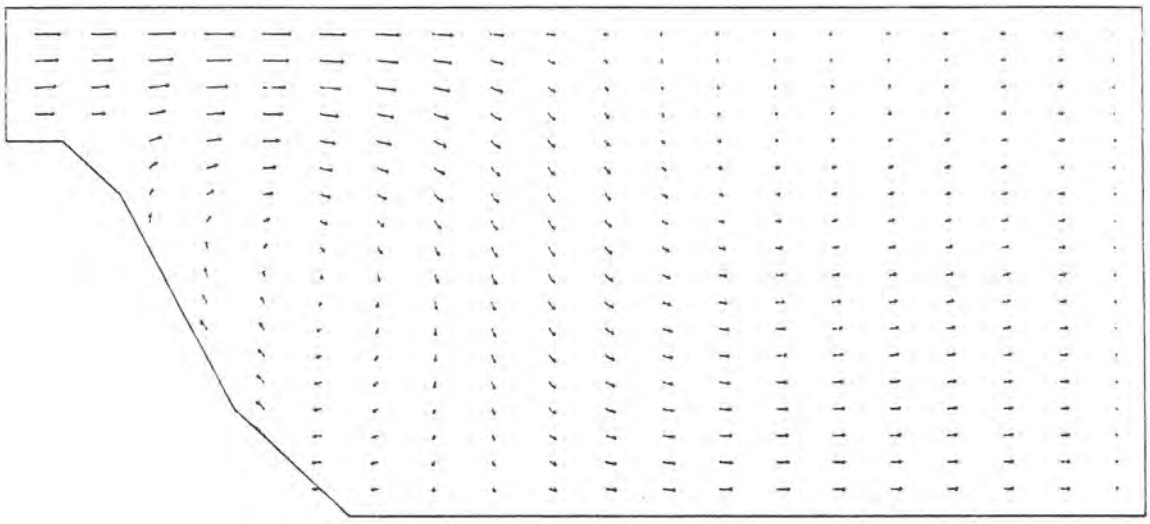

Figure 20. Plume with no heat loss to the atmosphere.

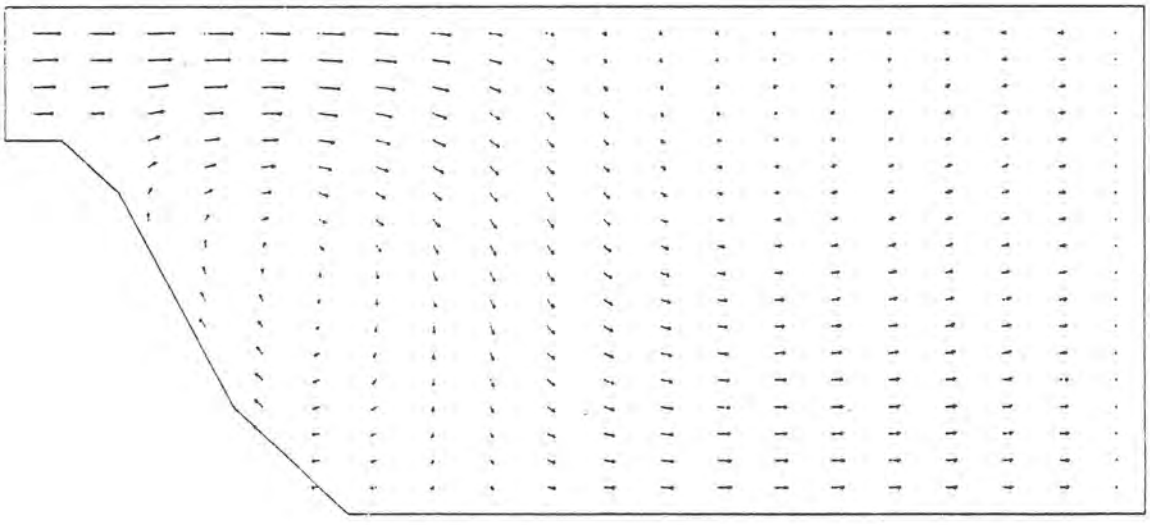

Figure 21. Plume with heat loss to the atmosphere.

In the velocity field, there appears only minor changes. (Fig 20, 21). Although, the changes will be probably more pronounced under conditions discussed above (smaller vertical diffusion coefficient), the instability, due to cooling at the surface if $T > T_{max}$, does not change the major pattern, especially because

the relevant time scale for heat lost to the atmosphere is much bigger than 6 hours. Cooling at the surface has to be included, however, if it is intended to verify a model against measurements.

The most difficult task is to model turbulent heat and momentum transport in the right way. Although the way they are modelled here is rather poor, the results obtained with different eddy coefficients used, indicate how sensitive the problem is to the right description of turbulence.

Using $K_V = A_V = 50$ cm^2/sec and $K_V = A_V = 10$ cm^2/sec respectively, results in isolines which do not look totally different (fig 22 and 23) but they indicate that there is a more pronounced spreading of warm water at the bottom if smaller eddy coefficients are used.

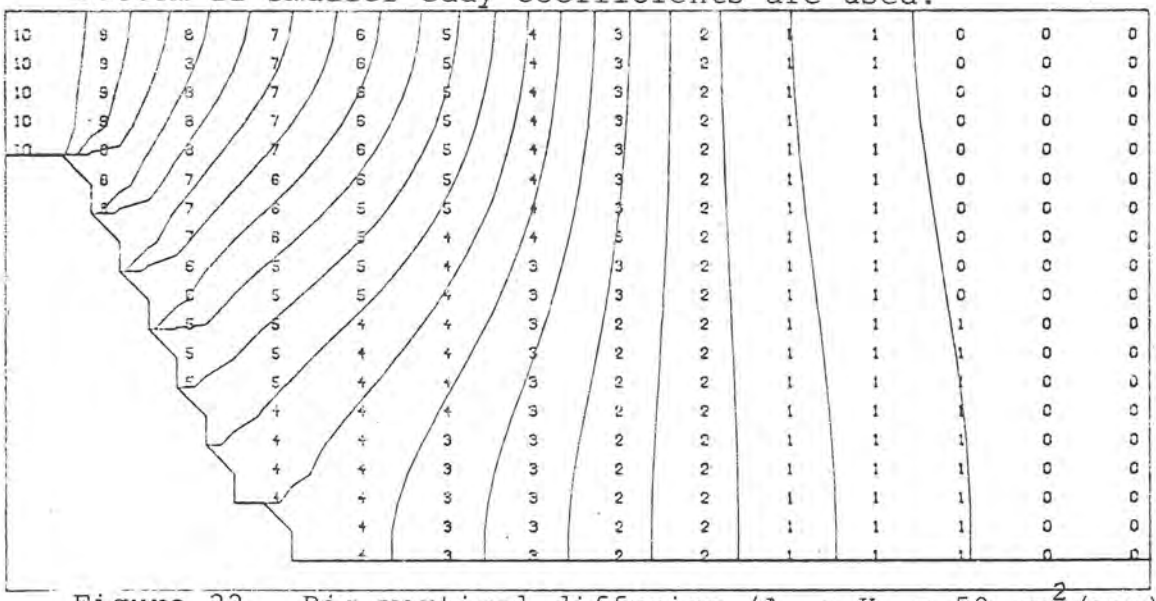

Figure 22. Big vertical diffusion ($A_V = K_V = 50$ cm^2/sec)

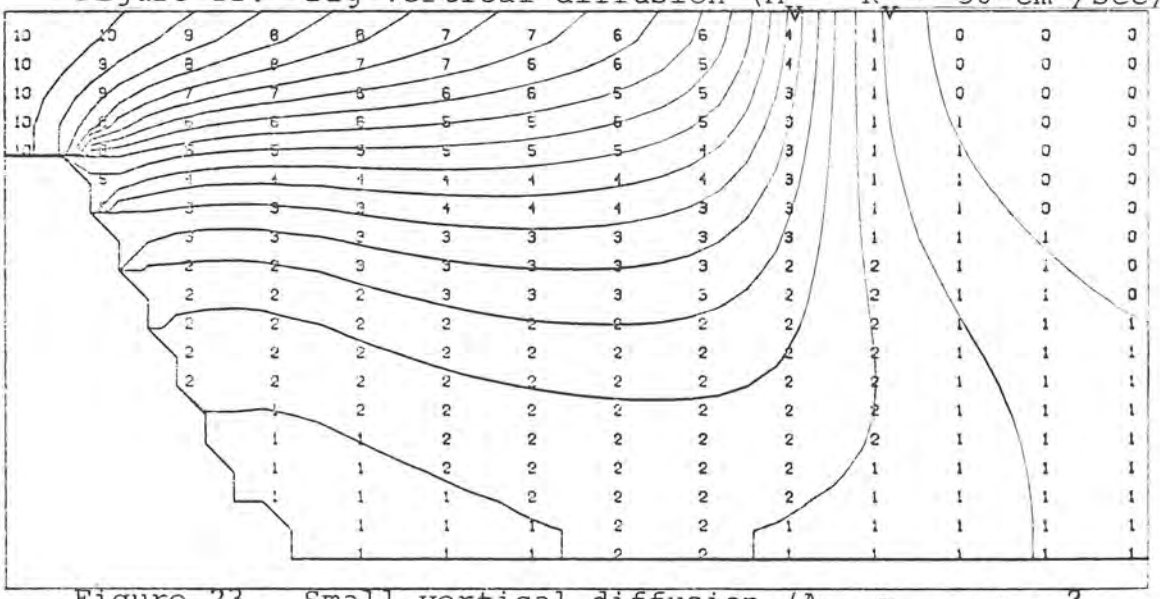

Figure 23. Small vertical diffusion ($A_V = K_V = 10$ cm^2

Comparing the velocities, however, shows $K_V = A_V = 50$ cm^2/sec causes a very weak and shallow zone of convergence (fig 24) and vertical velocity components of the order of 0.01 to 0.05 cm/sec over a long horizontal distance; in opposite to the second case, where vertical velocity components in the zone of convergence are between 0.1 and 0.2 cm/sec but restricted to a much smaller horizontal distance.

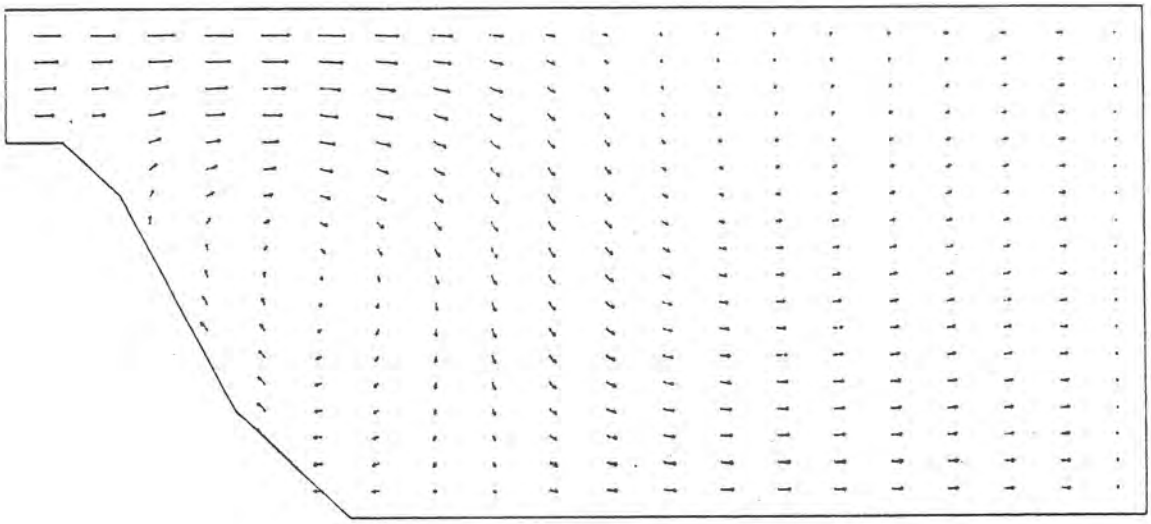

Figure 24. Big vertical diffusion ($A_V = K_V = 50$ cm^2/sec)

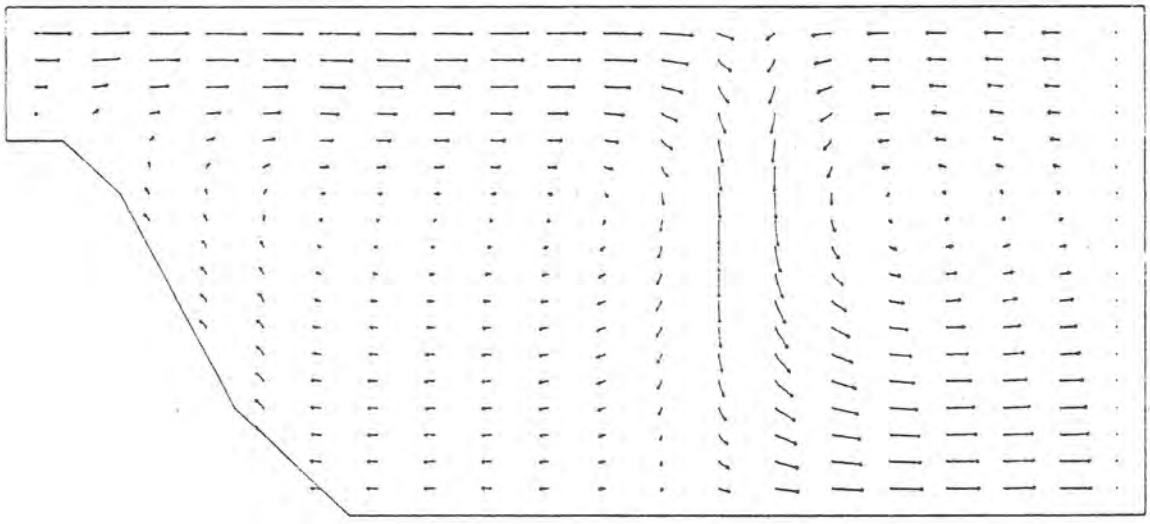

Figure 25. Small vertical diffusion ($A_V = K_V = 10$ cm^2/s)

Allowing higher eddy coefficients for unstable stratification than for stable stratification has about the same effect as using greater constant eddy coefficient, because the stratification is unstable for a large horizontal area (compare fig 26, 27 and 28, 29 respectively).

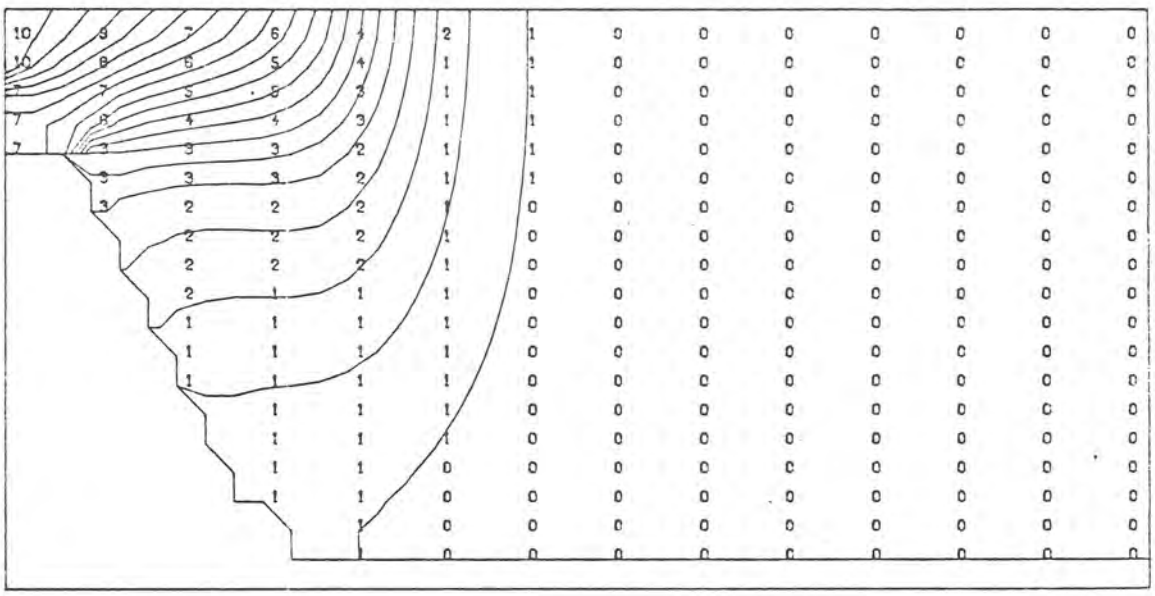

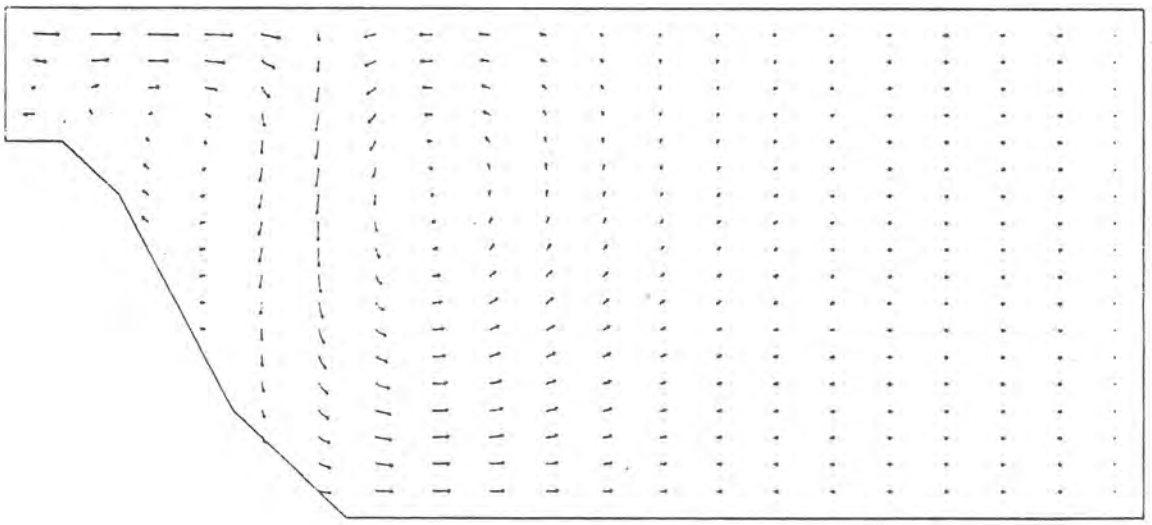

Figures 26, 27. Big eddy coefficient in areas with unstable stratification.

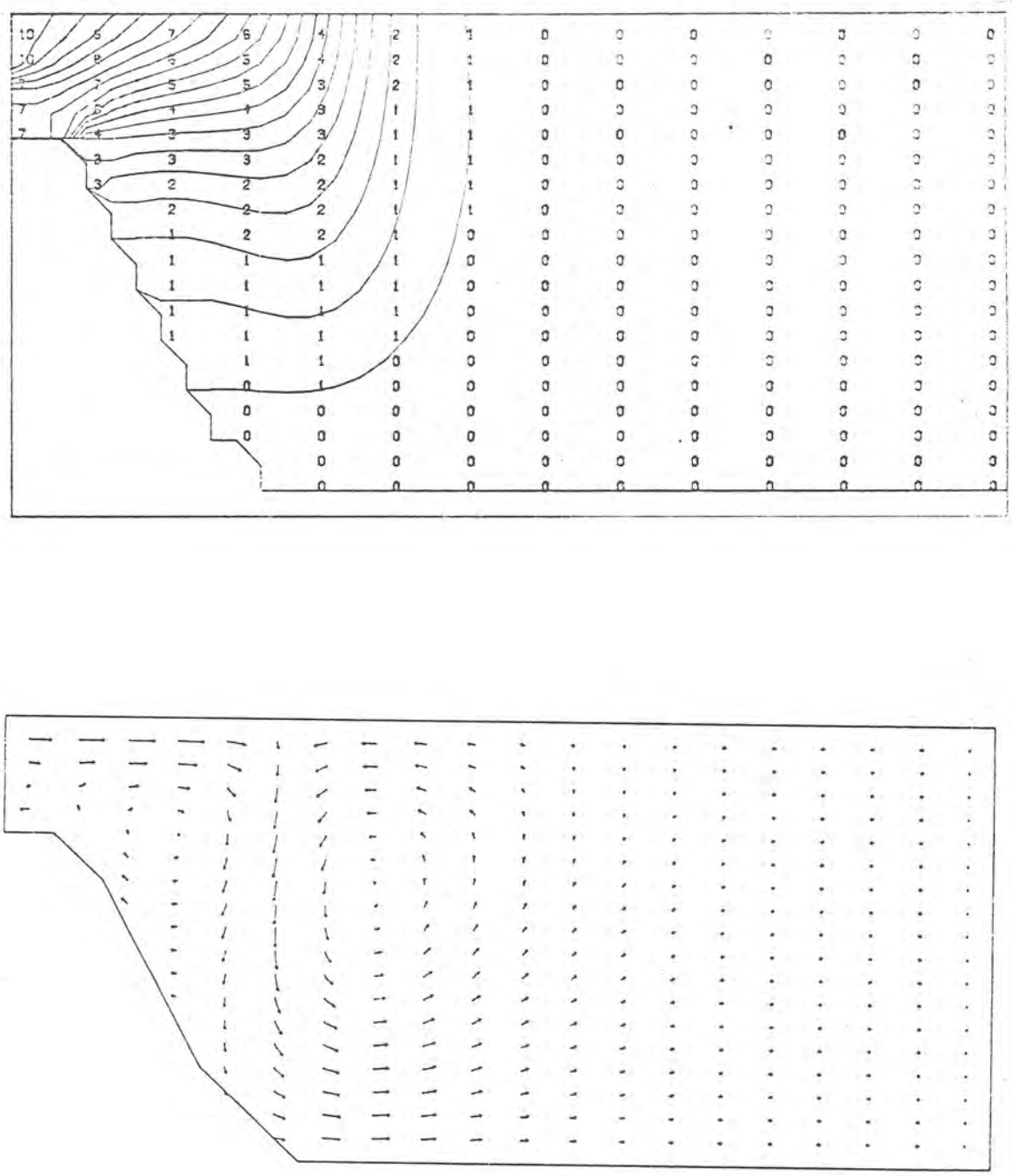

Figures 28, 29. Constant (small) eddy coefficient not depending on stratification.

Of the same importance as a proper model of vertical mixing, is a good assumption of horizontal diffusion, because the last experiment demonstrates that the zone of convergence appears about 100 m closer to the outlet if $A_h = K_h = 2.5$ m^2/sec is taken instead of $A_h = K_h =$ 5 m^2/sec. Furthermore the vertical velocity components double in size when the horizontal eddy coefficient is decreased to one half of its initial value (compare fig 31 to fig 33).

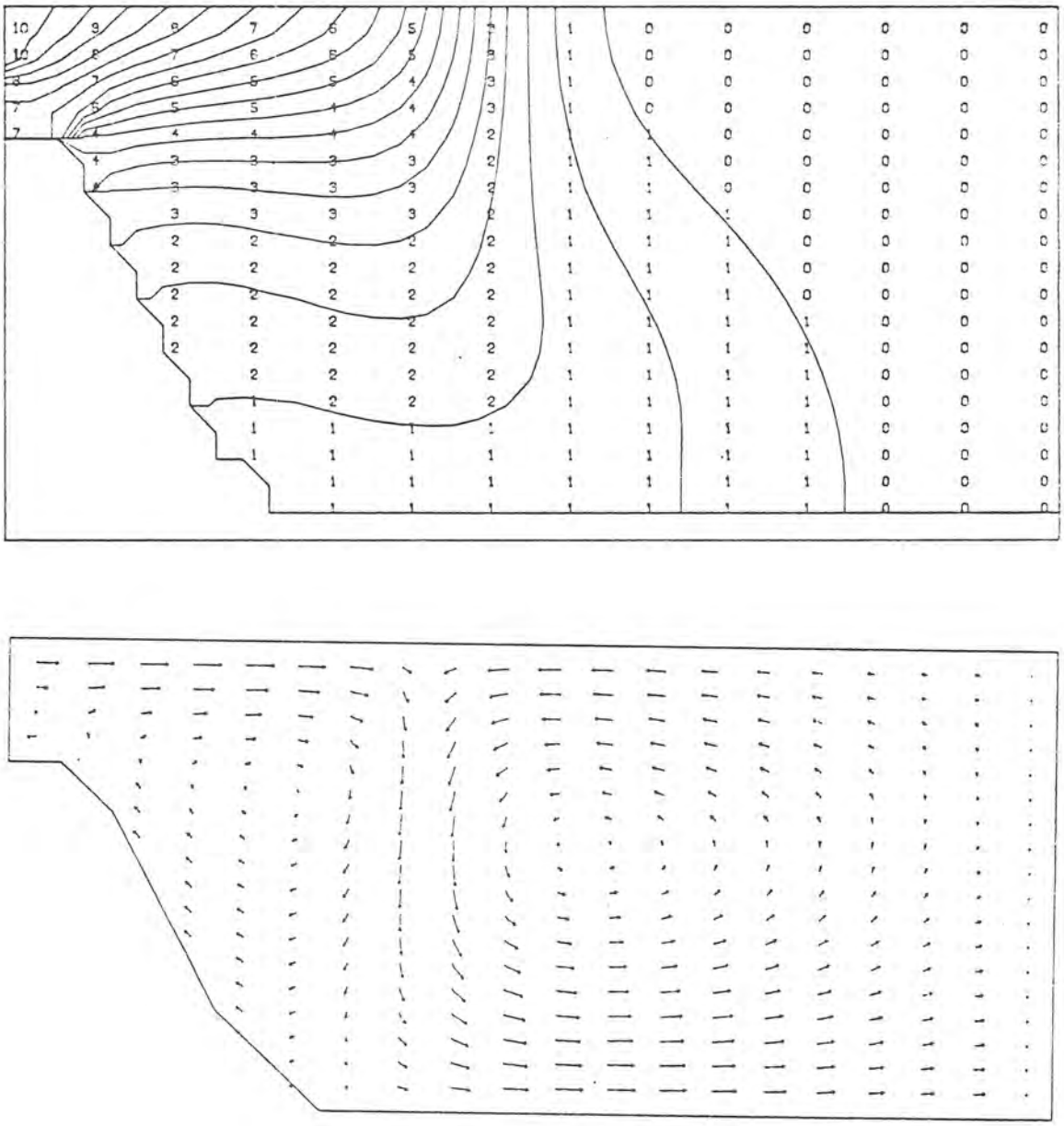

Figures 30, 31. Big horizontal diffusion coefficient $A_h = K_h = 5$ m^2/sec.

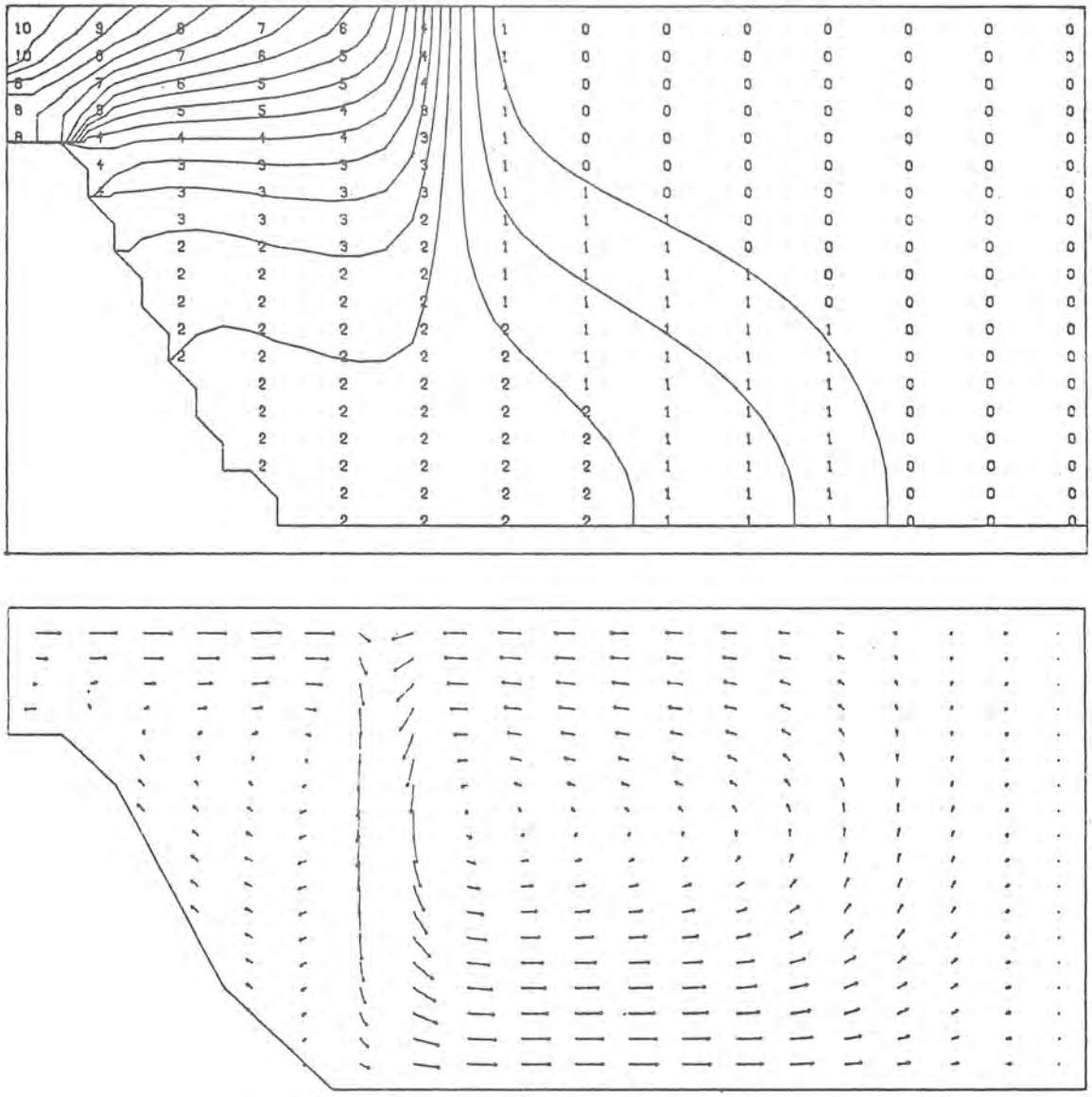

Figures 32,33. Small horizontal diffusion coefficient $A_h = K_h = 2.5\ m^2/sec.$

From the above discussion, it is obvious that a more advanced representation of the Reynold stresses and the turbulent heat flux is needed. Simple models for buoyancy-effected turbulence intend to handle mainly stable stratification by predicting the collapse of turbulence at a critical value of the flux Richardson number, defined by:

$$R_f = \frac{\text{Rate of turbulent energy removal by buoyant force}}{\text{Rate of turbulent energy creation by mean shear}}$$

For unstable flow, however, the Richardson number cannot be used as a parameter since no mean shear necessarily exists. More advanced models based on the solution of approximate transport equations for Reynold stresses and heat flux components require the solution of up to 12 coupled, nonlinear partial differential equations. A model which might be of practical importance is given by Gibson and Launder (1976). The turbulent fluxes are calculated from the local values of turbulent kinetic energy and its dissipation rate. The approach does not use the effective-viscosity concept, on which earlier k-ε models are based (applied for instance in Svensson 1976, reference H-H leden), by assuming $\nu_{eff} = c_\mu \frac{k^2}{\varepsilon}$.

Instead, algebreic formulas are solved for the turbulent fluxes as a function of k and ε, the transport of which is computed from partial differential equations. As simplifications, like predominantly horizontal flow, cannot be assumed, the solution of these equations becomes rather time consuming in 3 dimensions.

Therefore, time should be spent on their simplifications with respect to sinking plume modelling. A modification of the isotropic eddy coefficients, resulting from earlier k-ε models by some Richardson dependence, (compare Raithby 1976) is rather arbitrary.

Including such a turbulence model, Raithby´s model offers a cheap way to start 3-dimensional investigations of sinking plumes. Such investigations are nescessary, as fully 3-dimensionality is expected to alter the location of the zone of convergence and to change the temperature distribution in front of the zone of convergence. Basically, any differential-numerical model can handle sinking plume problems with a proper equation of state. The Paul-Lick model has already been applied to sinking plume problems (as mentioned in Dunn et al. 1975).

but Raithby´s model involves a better approximation of the advection terms and is in its simplicity, i.e. cheapness, more useful for basic 3-dimensional numerical studies.

REFERENCES

Dunn W E, Policastro A J, Paddock R A, (1975): Water Resources Research Program; Surface thermal plumes: evaluation of mathematical models for the near and complete field, Energy and Environmental Systems Division, Great Lakes Project, Part one.

Friedrich H, Levitus S, (1972): An approximation to the equation of state for sea water, suitable for numerical ocean model. J. of Ph. Oceanography, Vol. 2, No. 4.

Gibson M M, Launder B E, (1976): On the calculation of horizontal, turbulent, free shear flows under gravitational influence, Journal of Heat Transfer, February p. 81.

Krauss W,(1973): Methods and results of the theoretical oceanography, Vol. 1, Dynamics of the homogeneous and the quasihomogeneous ocean, Berlin.

Landau L D, Lifshitz E M, (1975): Fluid mechanics, Translated from the Russian. Course of theoretical physics. Vol.6, Oxford (1959) 1975.

Mehrotra S C, (1976): Turbulent Jets with Reversible Buoyancy (discussion), J. of the Hydraulics Div. Vol. 102, No. HY 4.

Monin A S, Yaglom A M, (1971): Statistical fluid mechanics, Mechanics of turbulence, Vol. 1, Cambridge, Mass., London.

Neumann G, Pierson W J Jr, (1966): Priciples of physical oceanography III, Englewood Cliffs, N.J.

Paul J F, Lick W J, (1974): A numerical model for a three-dimensionl variable-density jet, Division of Fluid, Thermal and Aerospace Seiences, Cleveland Ohio.

Pena M, Jain C, (1975): Turbulent Jets with Reversible Buoyancy, J. of the Hydraulics Div., Vol. 101, No HY 9.

Phillips N A, (1966): Boussinesq Approximation, Included in Thermal Convection: A Colloquium, National Center for Atmospheric Research, Boulder Colorado.

Raithby G D, (1976): Prediction of dispersion by surface discharge, Canada Center for Inland Waters, Canada.

Roache P J, (1972): Computational Fluid Dynamics, University of Kentucky, Kentucky.

Stern M E, (1975): Ocean circulation physics. International geophysics series, Vol. 19, New York.

Svensson U (1976): H-H leden. Rapport Nr 3001, Lund.

Thompsson P D, (1966): Thermal Convection: A Colloquium, National Center for Atmospheric Research, Boulder Colorado.

Turner J S, (1973): Buoyancy effects in fluids, Cambridge at the University Press.

Wilmot W, (1976): A numerical model of the effects of reactor cooling water on fjord circulation, SMHI Rapporter, No. RHO 6.

Wilmot W, Svensson J, (1977): Beräkningar av effekten av en sänktunnel på cirkulationen i Öresund, SMHI.

Notiser och preliminära rapporter

Serie HYDROLOGI

Nr 1 Sundberg-Falkenmark M
Om isbärighet. Stockholm 1963

Nr 2 Forsman, A
Snösmältning och avrinning. Stockholm 1963

Nr 3 Karström, U
Infrarödteknik i hydrologisk tillämpning: Värmebilder som hjälpmedel i recipientundersökningar. Stockholm 1966

Nr 4 Moberg, A
Svenska sjöars isläggnings- och islossningstidpunkter 1911/12-1960/61. Del 1. Redovisning av observationsmaterial. Stockholm 1967

Nr 5 Ehlin, U & Nyberg, L
Hydrografiska undersökningar i Nordmalingsfjärden. Stockholm 1968

Nr 6 Milanov, T
Avkylningsproblem i recipienter vid utsläpp av kylvatten. Stockholm 1969

Nr 7 Ehlin, U & Zachrisson, G
Spridningen i Vänerns nordvästra del av suspenderat materiel från skredet i Norsälven i april 1969. Stockholm 1969

Nr 8 Ehlert, K
Mälarens hydrologi och inverkan på denna av alternativa vattenavledningar från Mälaren. Stockholm 1970

Nr 9 Ehlin, U & Carlsson, B
Hydrologiska observationer i Vänern 1959-1968 jämte sammanfattande synpunkter. Stockholm 1970

Nr 10 Ehlin, U & Carlsson, B
Hydrologiska observationer i Vänern 17-21 mars 1969. Stockholm 1970

Nr 11 Milanov, T
Termisk spridning av kylvattenutsläpp från Karlshamnsverket. Stockholm 1971

Nr 12 Persson, M
Hydrologiska undersökningar i Lappträskets representativa område. Rapport I. Stockholm 1971

Nr 13 Persson, M
Hydrologiska undersökningar i Lappträskets representativa område. Rapport II. Snömätningar med snörör och snökuddar Stockholm 1971

Nr 14 Hedin, L
Hydrologiska undersökningar i Velens representativa område. Beskrivning av området, utförda mätningar samt preliminära resultat. Rapport I. Stockholm 1971

Nr 15 Forsman, A & Milanov, T
Hydrologiska undersökningar i Velens representativa område. Markvattenstudier i Velenområdet. Rapport II. Stockholm 1971

Nr 16 Hedin, L
Hydrologiska undersökningar i Kassjöåns representativa område. Nederbördens höjdberoende samt kortfattad beskrivning av området. Rapport I. Stockholm 1971

Nr 17 Bergström, S & Ehlert, K
Stochastic Streamflow Syntheses at the Velen representative Basin. Stockholm 1971

Nr 18 Berström, S
Snösmältningen i Lappträskets representativa område som funktion av lufttemperaturen. Stockholm 1972

Nr 19 Holmström, H
Test of two automatic water quality monitors under field conditions. Stockholm 1972

Nr 20 Wennerberg, G
Yttemperaturkartering med strålningstermometer från flygplan över Vänern under 1971. Stockholm 1972

Nr 21 Prych, A
A warm water effluent analyzed as a buoyant surface jet. Stockholm 1972

Nr 22 Bergström, S
Utveckling och tillämpning av en digital avrinningsmodell. Stockholm 1972

Nr 23 Melander, O
Beskrivning till jordartskarta över Lappträskets representativa område. Stockholm 1972

Nr 24 Persson, M
Hydrologiska undersökningar i Lappträskets representativa område. Rapport III. Avdunstning och vattenomsättning. Stockholm 1972

Nr 25 Häggström, M
Hydrologiska undersökningar i Velens representativa område. Rapport III. Undersökning av torrperioderna under IHD-åren fram t o m 1971. Stockholm 1972

Nr 26 Bergström, S
The application of a simple rainfall-runoff model to a catchment with incomplete data coverage. Stockholm 1972

Nr 27 Wändahl, T & Bergstrand, E
Oceanografiska förhållanden i svenska kustvatten. Stockholm 1973

Nr 28 Ehlin, U
Kylvattenutsläpp i sjöar och hav. Stockholm 1973

Nr 29 Andersson, U-M & Waldenström, A
Mark- och grundvattenstudier i Kassjöåns representativa område. Stockholm 1973

Nr 30 Milanov, T
Hydrologiska undersökningar i Kassjöåns representativa område. Markvattenstudier i Kassjöåns område. Rapport II. Stockholm 1973

SMHI Rapporter

HYDROLOGI OCH OCEANOGRAFI

Nr RHO 1
Weil, J G
Verification of heated water jet numerical model
Stockholm 1974

Nr RHO 2
Svensson, J
Calculation of poison concentrations from a hypothetical accident off the Swedish coast
Stockholm 1974

Nr RHO 3
Vasseur, B
Temperaturförhållanden i svenska kustvatten
Stockholm 1975

Nr RHO 4
Svensson, J
Beräkning av effektiv vattentransport genom Sunninge sund till Byfjorden
Stockholm 1975

Nr RHO 5
Bergström, S & Jönsson, S
The application of the HBV runoff model to the Filefjell research basin
Norrköping 1976

Nr RHO 6
Wilmot, W
A numerical model of the effects of reactor cooling water on fjord circulation
Norrköping 1976

Nr RHO 7
Bergström, S
Development and Appl. of a Conceptual Runoff Model
Norrköping 1976

Nr RHO 8
Svensson, J
Seminars at SMHI 1976-03-29--04-01 on Numerical Models of the Spreading of Cooling-water
Norrköping 1976

Nr RHO 9
Simons, J & Funkquist, L & Svensson, J
Application of a numerical model to Lake Vänern
Norrköping 1977

Nr RHO 10
Svensson, S
A statistical study for automatic calibration of a conceptual runoff model
Norrköping 1977

Nr RHO 11
Bork, I
Model studies of dispersion of pollutants in Lake Vänern
Norrköping 1977

Nr RHO 12
Fremling, S
Sjöisars beroende av väder och vind, snö och vatten
Norrköping 1977

SMHI Rapporter

HYDROLOGI OCH OCEANOGRAFI

Nr RHO 13 Fremling, S
Sjöisars bärighet vid trafik.
Norrköping 1977

Nr RHO 14 Bork, I
Preliminary model studies of sinking plumes.
Norrköping 1978